Karami et al., *BioImpacts.* 2025;15:24196
doi: 10.34172/bi.24196
https://bi.tbzmed.ac.ir/

Anti-Alzheimer effects of the newly synthesized cationic compounds as multi-target dual hAChE/hBuChE inhibitor: An *in silico*, *in vitro*, and *in vivo* approach

Hosna Karami[1], Somaieh Soltani[2*], Gerhard Wolber[3], Saeed Sadigh-Eteghad[4], Roghaye Nikbakht[5], Hanieh Farrokhi[5], Farzaneh Narimani[2], Reza Teimuri-Mofrad[5], Mohammad-Reza Rashidi[2,6*]

[1]Higher Education Institute of Rab-Rashid, Tabriz, Iran
[2]Pharmacy Faculty, Tabriz University of Medical Sciences, Tabriz, Iran
[3]Molecular Design Group, Pharmaceutical and Medicinal Chemistry, Institute of Pharmacy, Freie Universität Berlin, Germany
[4]Neurosciences Research Center, Tabriz University of Medical Sciences, Tabriz, Iran
[5]Department of Organic and Biochemistry, Faculty of Chemistry, University of Tabriz, 51666-16471, Tabriz, Iran
[6]Nanotechnology Research Center and Pharmacy Faculty, Tabriz University of Medical Sciences, Tabriz, Iran

Article Info

Article Type:
Original Article

Article History:
Received: 5 Dec. 2021
Revised: 29 Apr. 2024
Accepted: 30 Apr. 2024
ePublished: 29 Dec. 2024

Keywords:
Alzheimer's disease therapeutics,
Multi-target neuroprotective,
Cholinesterase inhibitors,
Amyloid-beta interventions,
Neuromolecular mechanisms,
Aβ treated rat cognition improvement

Abstract

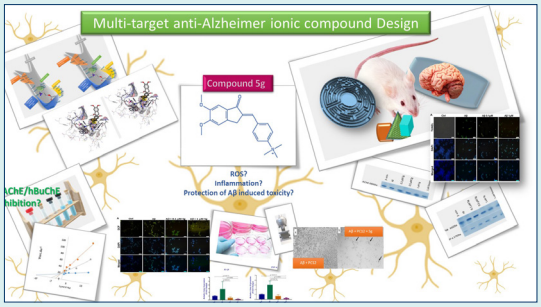

Introduction: Multi-target anti-Alzheimer's disease (AD) compounds are promising leads for the development of AD modifying agents. Ionic compounds containing quaternary ammonium moiety were synthesized, and their multi-targeted anti-AD effects were examined.

Methods: Imidazole derivatives containing a quaternary ammonium moiety were synthesized and evaluated for their potential anti-Alzheimer properties using computational (*in silico*), cellular (*in vitro*), and animal (*in vivo*) models. The inhibition kinetics of both human acetylcholinesterase (hAChE) and butyrylcholinesterase (hBuChE) were assessed. Neuroprotective effects in amyloid-beta (Aβ)-exposed PC12 cells were also examined. Furthermore, the compounds' impact on Aβ-induced memory impairment in Wistar rats was evaluated, with a detailed analysis of the underlying mechanisms.

Results: Compound 5g demonstrated acceptable cytotoxicity against human cells. This compound exhibited non-competitive dual inhibition of both hAChE and hBuChE. Additionally, compound 5g mitigated the morphological changes induced by amyloid-beta (Aβ) in PC12 cells and decreased cell mortality. It exhibited anti-oxidative stress properties, evident by reduction in reactive oxygen species (ROS) production, and inhibition of lipid peroxidation. The compound also down regulated the expression of pro-inflammatory genes IL-1β and TNF-α. In vitro studies validated compound 5g's ability to inhibit lactate dehydrogenase (LDH), attenuate neuroinflammation, and prevent the autophagy-apoptosis cascade. When administered to rats with Aβ-induced memory dysfunction, compound 5g enhanced cognitive function and improved spatial memory. In the hippocampi of treated rats, there was a noted downregulation of TNF-α and NF-kB. Furthermore, compound 5g counteracted the elevated activity of AChE. Molecular modeling validated the binding of compound 5g to both steric and catalytic sites of cholinesterase enzymes.

Conclusion: The novel quaternary ammonium derivative, compound 5g, demonstrated multi-target anti-AD properties, as evidenced by *in silico*, *in vitro* and *in vivo* studies. Behavioral assessments and molecular analyses further confirmed its therapeutic efficacy in amyloid-beta (Aβ)-challenged rats.

Introduction

Alzheimer's disease (AD) is a chronic neurodegenerative disease known mainly for short-term memory loss, neuronal misfunctions, and gradual death.[1,2] The

*Corresponding authors: Somaieh Soltani, Email: soltanis@tbzmed.ac.ir; Mohamad-Reza Rashidi, Email: rashidi@tbzmed.ac.ir

accumulation of amyloid-beta (Aβ) plaques around neurons, hyperphosphorylation of microtubules-associated Tau protein, intracellular neurofibrillary tangles (NFT), and the reduction of acetylcholine (ACh) level in the synaptic cleft have been reported as main hallmarks of AD.[3-7] The disintegration of axons, degenerative dysfunction of synapsis, neuroinflammation, dysregulation of membranes, and dysfunction of brain metabolic pathways has been reported as underlying mechanisms of AD initiation and progression.[1,2,8] Oxidative stress and free radical formation, metal dys-homeostasis, excitotoxic processes beyond many AD-associated genes are known as events affecting AD progression rate.[9]

The current FDA-approved drugs are anticholinesterase inhibitors (donepezil, rivastigmine, and Galantamine)[10,11] and NMDA antagonists (Memantine). Due to the symptomatic relevant characteristics of these drugs and the feedback mechanisms that prevent the long-term effectiveness of enzyme inhibitors, the available drugs can not contribute to AD modification. Consequently, researchers try to develop anti-AD disease-modifying agents (DMA) considering the complex nature of AD hallmarks.

Multi-targeted drugs (MTD) can act as DMAs. MTDs interact weakly with multiple AD-associated targets and increase potency against acetylcholinesterase (AChE)/ butyrylcholinesterase (BuChE), Aβ plaque, and Tau tangle formation. At the same time, they possess antioxidant activity, neuroprotective effect, metal-complex forming property, antagonism of voltage-dependent calcium channel, inhibition of glutamate-induced excite-toxicity, and β-secretase (BACE1) enzyme, antagonizing histamine H_3 receptor and cannabinoid CB1 receptor.[12]

hAChE plays a dominant role in brain health.[13] Evidence has shown that the activity of hBuChE increases during AD.[10,13] Inhibition of both hAChE and hBuChE is one of the recently emerged approaches for AD treatment.[10,13] Different studies suggested non-cholinergic functions for hAChE.[14,15] hAChE-Aβ complexes promote the formation of Aβ fibrils[14,15] that increase neurotoxicity. Selective inhibition of hBuChE has some advantages due to the absence of hBuChE-Aβ toxic complexes. The development of the selective hBuChE[10,13] with the ability to interact with the active and the peripheral sites of hAChE[16,17] has been reported previously. Donepezil (an indanone derivative) interacts with both active and peripheral sites of hAChE (Fig. 1).

Positive charge centers such as quaternary ammonium facilitate the interaction of AChE/BuChE inhibitors with the active site. In contrast, the lower penetration of the permanently charged quaternary ammonium from the blood-brain barrier[18] limited their application as functional groups in such drugs. Some permanently charged quaternary ammonium-containing molecules were designed and investigated mainly as the peripheral

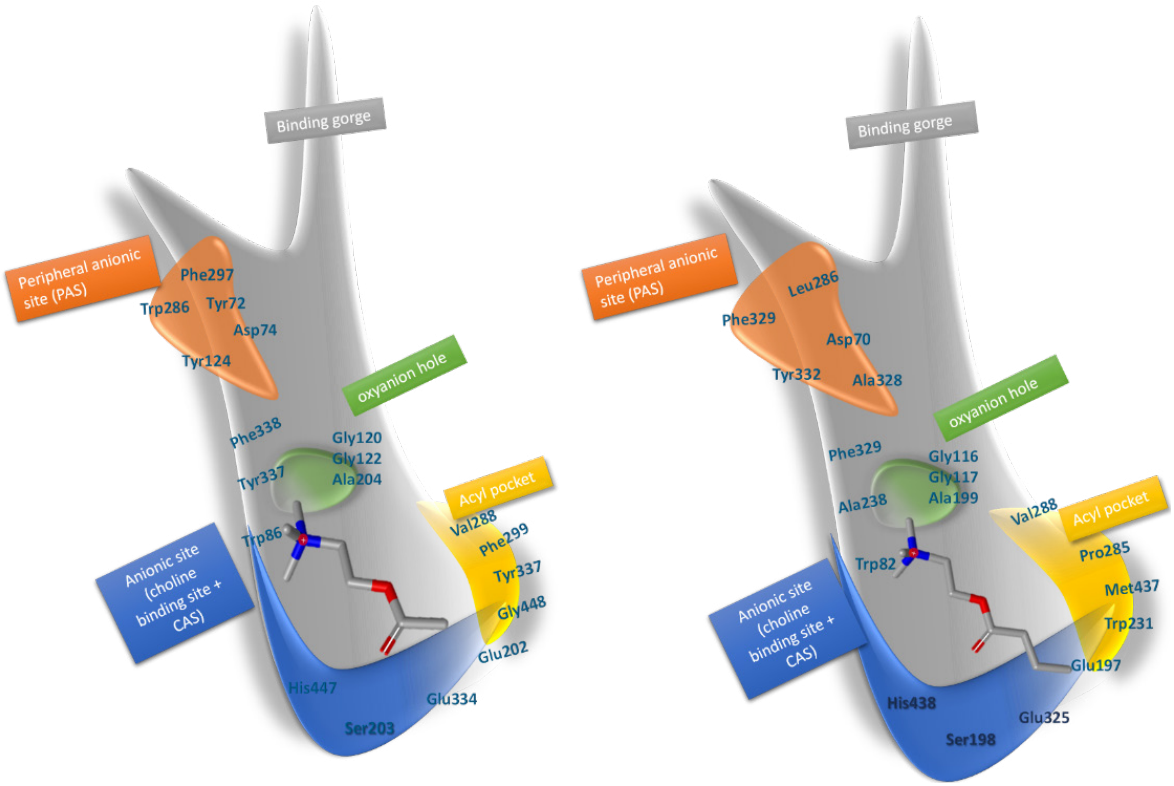

Fig. 1. Schematic overview of the binding gorge of hAChE (left) and hBuChe (right). The catalytic site of enzymes including the anionic site (similar triad amino acids), acyl pocket (larger in hBuChe), oxi anionic hole (similar), and preferable binding pocket (including aromatic amino acids in hAChE and nonaromatic amino acids in hBuChE) are obvious in schematic view. (residue numbers are for 4EY7 and 4BDS pdb codes).

inhibitor of ChE to be utilized in myasthenia gravis.[19,20] Recent investigations suggested a promising route for the delivery of positively charged drugs to the CNS.[21,22] Choline transporters have been reported to transport donepezil and certain permanently charged compounds to the CNS.[23-26] Incorporation of para-quaternary ammonium moieties on the benzene ring has resulted in the dual-site inhibition of hAChE and hBuChE,[27] water solubility improvement[28] and enhanced choline transporter binding capability.[23] Some piperazenium derivatives were introduced and their biological activities against AD were evaluated in our recent papers.[25,29]

Two newly-designed derivatives, including quaternary ammonium substitution (Fig. 2) along with other derivatives from our previous paper[30,31] were investigated for their dual AChE/BuChE inhibition activity. The SAR of the synthesized molecules toward hAChE and hBuChE inhibitory activity was investigated using molecular docking and pharmacophore mapping methods. The anti-AD activity of the most potent AChE/BuChE inhibitor compound with quaternary ammonium moiety was investigated in the current study by evaluating its biological activity toward several AD-related targets. Cytotoxicity of the selected inhibitors was studied on MCF7, B16, and PC12 cell lines using MTT assay.[32] The neuroprotective effect against Aβ-induced toxicity of PC12 cell toxicity was investigated, while the expression of proinflammatory cytokines in PC12 cells and the rat brain was also studied. Additionally, in vivo studies assessed the efficacy of selected compounds on Aβ-induced memory impairment in Wistar rats, serving as an AD rat model.

Materials and Methods

Synthesizing of the compounds 5g and 5i

The details of derivatives synthesizing and molecular structure characterizing were reported in our previous papers.[30,31] Compounds 5g and 5i were synthesized in the current study, and their characterizations results are as follows:

2-[4-(N,N,N-trimethylammonium)benzilidine]-5,6-dimethoxy-2,3-dihydro-1H-inden-1-one (5i)

Compound **5h** (1mmol) was dissolved in acetone (14cc) then CH_3I (3mmol) was added. The reaction mixture was

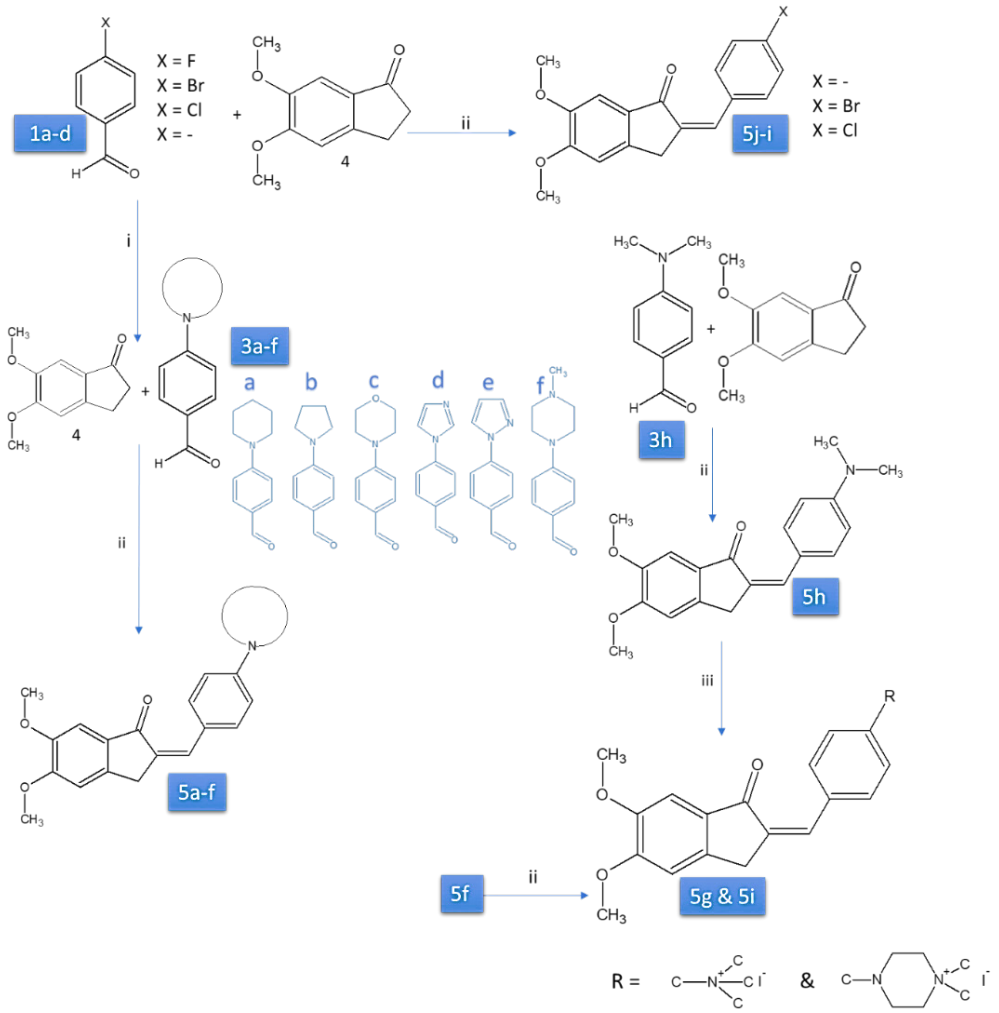

Fig. 2. Synthesis of compounds 5a-l (compounds 5g and 5i designed and synthesized in the current study other derivatives were reported in our previous publications).[21,22]

stirred 48h at 30 °C. The solid was filtered and washed with acetone. Residual solvent was removed under reduced pressure to afford compound **5i** as yellow solid; Yield 75%; Mp = 282-284 °C; FT-IR (KBr) ν 3000, 3039, 1686, 1632, 1496, 1300,1088, 836 cm^{-1}; ^1H NMR (400MH_Z, $CDCl_3$) δ 3.64(9H, s, ^+N-CH_3), 3.84 (3H, s, O-CH_3), 3.91 (3H, s, O-CH_3), 4.05(2H, s, inden-CH_2), 7.23 (1H, s, Ar-H), 7.24 (1H, s, Ar-H), 7.50(1H, s, methine-H), 7.97-7.99 (2H, d, *J* = 8.95 Hz, Ar–H), 8.06- 8.08 (2H, d, *J* = 8.98 Hz, Ar–H), ppm; ^{13}C NMR (100 MHz, DMSO): δ 30.69, 31.32, 55.70, 56.04, 104.56, 104.61, 108.07, 120.11, 121.12, 128.64, 129.74, 131.54, 136.76, 138.18, 145.36, 147.14, 149.43, 155.58, 191.61 ppm.

2-[4-(N,N-dimethylpipyrazinoammonium)benzylidine]-5,6-dimethoxy-2,3-dihydro-1H-inden-1-one (5g)

Compound **5f** (1mmol) was dissolved in acetone (14cc) then CH_3I (3mmol) was added. The reaction mixture was stirred 48h at 30 °C. The solid was filtered and washed with acetone. In conclusion, the residual solvent was removed under reduced pressure to afford compound 5g as a yellow solid. Yield 82%; mp: 182-184 °C; FT-IR (KBr) ν 2924, 1674, 1302, 1222, 1090, 896 cm^{-1}; ^1H NMR (400MH_Z, DMSO) δ 3.22 (6H, s, ^+N-CH_3), 3.56-3.58 (4H, m, piperazino-CH), 3.63-3.67 (4H, t, J = 8Hz, piperazino-CH), 3.82 (3H, s, O-CH_3), 3.89 (3H, s, O-CH_3), 3.93 (2H, s, inden-CH_2), 7.10-7.12 (2H, d, *J* = 8.68 Hz, Ar–H), 7.18 (1H, s, Ar-H), 7.21 (1H, s, Ar-H), 7.36 (1H, s, methine-H), 7.64-7.67 (2H, d, *J* = 8.85 Hz, Ar–H), ppm; ^{13}C NMR (100 MHz, DMSO): δ 31.71, 40.09, 50.36, 55.66, 56.00, 59.95, 104.40, 104.48, 108.11, 115.07, 126.05, 130.30, 131.29, 132.05, 132.58, 149.24, 149.94, 154.96, 191.87 ppm.

hAChE and hBuChE inhibition assay

Materials and equipment

5,5′-Ditiobis(2-nitrobenzoic acid (DTNB) and acetylthiocholine iodide (ATCI) were purchased from Acros. Butyrylthiocholine iodide (BuTCI) was purchased from TCI Europe. Di-sodium hydrogen phosphate and hydrochloridric acid were obtained from Merck. Spectrophotometric measurements were performed by Shimadzu UV/2550 Spectrophotometer equipped with a thermocycler bath.

Extraction of hAChE and hBuChE from human blood

The blood samples obtained from a healthy volunteer were approved by local ethics (IR.TBZMED.REC.868). The blood sample (2.0 mL) was collected in a heparinized tube and mixed with 8.0 mL of sodium phosphate buffer (0.1 M, pH 7.4)). The mixture was centrifuged (5 minutes at 3000 g) and washed with 2-3 volumes of normal saline. After centrifugation and washing three times, 0.1 ml of the packed RBC was transferred to another tube. To obtain the hemolysate, 6.0 mL of distilled water was added to RBC, and the mixture was centrifuged (1000 g) after 5 minutes of incubation in ice. Aliquots of the erythrocyte membranes were stored at -20 °C until use.[33,34] ChE activity was measured before analysis.

hAChE and hBuChE inhibition assay

Modified Ellman's method was performed to measure ChE activity.[35] All synthesized compounds, donepezil, and galantamine, were weighed and dissolved in DMSO (to prepare 10^{-3} M stock solutions). To prepare the working standards (10^{-4}-10^{-9} M), stock solutions were diluted in 100 mM phosphate buffer (pH 8.0). The final concentration of DMSO in the working solutions was less than 1.3 (V/V %).

To investigate the anticholinesterase activity of compounds, 550 µL phosphate buffer solution (100 mM, pH 8.0), 150 µL DTNB solution (0.5 mM), 150 µL of the studied compound solution, and 150 µL ATCI solution (1.0 mM) (for hAChE) were added to test cuvette (1 mL). The mixture was gently shacked and incubated at 37 °C for 5 min. The reaction was begun by adding 50 µL of the hemolysate to the test cuvette (the total volume of the mixture was 1050 µL). Absorbance was monitored at the wavelength of 412 nm over 10 min. The same method described was applied for hBuChE inhibition assay, while instead of ATCI, BuTCI was used.

Double reciprocal equation (log [inhibitor concentration] vs. the percentage of inhibition) was used to calculate the IC_{50} values.

Kinetic study

The inhibition assay was done at 4 different concentrations of ACTI (0.06-1.0 mM). The velocity of the enzymatic reaction was measured with two different inhibitor concentrations (that showed 30-70% inhibition) and without an inhibitor. To obtain inhibition constants (k_i) of hAChE, double reciprocal plots (Lineweaver–Burk plot) of 1/V vs. 1/[S] were applied. Also, we calculated non-competitive inhibition constants ($K_{i'}$) using the plot of $1/V_{app}$ vs. inhibitor concentration.[36]

Molecular modeling study

Docking studies were done using the Gold software. The crystal structures of hAChE (PDB code: 4EY7) and hBuChE (PDB code: 4BDS) were downloaded from the protein data bank (http://www.rcsb.org).

Before docking, co-crystallized inhibitors and unnecessary water molecules were extracted from the crystal structure, and polar hydrogens were added using the protein preparation module of gold software. The binding mode of donepezil was studied using Ligand-Scout software, and the binding pocket and pharmacophores were calculated. The binding cavity was designed according to the binding mode of the compounds to the enzymes. The obtained information from literature about the important amino acids for interaction in the binding gorge. Studied molecules were docked against the desired

enzymes using the gold-score method followed by a chem score re-docking procedure. The best conformer was visualized using ligands out software.

To validate the developed docking method, the co-crystallized compounds i.e. donepezil, and butyrylthiocholine, respectively, for 4EY7 and 4BDS, were removed, and the drawn structures were docked against the designed binding cavity. The resulting conformers were superimposed onto the original co-crystallized compound, and the orientation and mode of interaction were investigated. The obtained RMSD values were regarded as error criteria of the docking procedure. The results showed that the developed docking method was done by RMSD values of less than 2.0 A°.

Cell viability assay (MTT assay)

To study the effect of the compounds 5g, 5f, galantamine, and donepezil on cell viability, we selected normal and cancerous human cell lines MCF7 is a breast cancer cell line and B16 is a murine tumor cell line used for research as a human skin cancer cell line. Additionally, to assess the potential neuroprotective attributes of the compound 5g, PC12 cells were selected. PC12 cells are rat pheochromocytoma cells known for their suitability in studies related to neuronal cell properties. Before neuroprotection evaluations, the toxic effects of compounds 5g, 5f, galantamine, and donepezil on PC12 cells were assessed using the MTT assay. All cell lines were sourced from the Pasteur Institute of Iran.

MTT assay is a colorimetric method to evaluate the viability of cells. The reduction of MTT in the mitochondria of living cells leads to the production of a formazan product with a purple or violet color, which is not soluble in water.[32] For the MTT method, the cells were passaged in RPMI 1640 with 10% FBS (Gibco, Grand Island, NY, USA). After cell culture, cells were separated with trypsin- EDTA of the flask. (Gibco, Grand Island, NY, USA). 200 microliters of a cell suspension containing 10^4 cells per well of 96-well plates load, and for 24 hours at 37 °C, the concentration of 5% CO_2 and appropriate humidity were pre-incubated. Then, cells were exposed to different concentrations of compounds, and MTT (Sigma-Aldrich) solution with 5 mg/mL concentration for 48 and 4 hours was placed, respectively. 200 microliters of DMSO (Merck- Germany) and 25 ml Sorensen's buffer as reaction stopper were added to each plate. The plate was located on a plate stirring device after 40 minutes. Elisa plate reader measured absorption at 570 nm. The data were analyzed by GraphPad Prism 7 software. For validation of this method, positive control (culture medium and cells) and negative control (culture medium, cells, and DMSO) were placed.

PC12 Cell culture for neuroprotection study

PC12 cells were used to investigate the neuroprotective effect of compound 5g on neurotoxicity. The culture medium was RPMI 1640 medium that contained 10% horse serum, 5% fetal calf serum, and gentamicin 50 mg/ml. Plastic flasks were coated with 0.03% poly-L-ornithine and were used to incubate monolayer cultures (density = 0.1 to 0.3×10^6 cells/cm^2) in a 95% air, 5% CO_2 and humidified atmosphere at 37 °C. The culture medium was refreshed every 48 h. PC12 cells that were grown on 10-cm dishes were exposed to 5 μM Aβ (1-42) (rat/mouse, ab120959) in the presence or the absence of compound 5g at two concentrations (0.1 and 1.0 μM).

Simultaneous DCFH-DA assay and DAPI staining

2′,7′-Dichlorofluorescein-diacetate (DCFH-DA) was utilized to assess the ROS level in cells. For the DCFH-DA assay, cells from the studied groups were treated with 10 μM DCFH-DA. To ensure that DCFH-DA was incorporated into all membrane-bound vesicles, the treated cells were incubated for 15 minutes at room temperature. This period allows esterase enzymes in the cells to cleave the di-acetate groups, converting DCFH-DA into DCF. The fluorescence of DCF was then quantified using a Thermo Scientific-Finland Multiscan spectrophotometer (GO MULTISCAN) with an excitation at 485 nm and emission at 530 nm.

To further assess DCF localization in cell nuclei, cells were counterstained with DAPI (4′,6-diamidino-2-phenylindole), a fluorescent dye that preferentially binds to adenine–thymine-rich regions in DNA. The DAPI-stained cells were visualized using a fluorescence microscope set to an excitation of 358 nm and an emission of 461 nm.

TUNEL assay

For performing the terminal deoxynucleotidyl transferase dUTP nick end labeling (TUNEL) assay, control, and treated cells were transferred to slides and exposed to PBS buffer (containing 4% paraformaldehyde, pH 7.4) for 1 h at room temperature. The obtained slides were rinsed with PBS and incubated in the blocking solution (methanol 3% in H_2O_2) for 10 minutes. Then they incubated with 0.1% Triton X-100 in 0.1% sodium citrate for 2 minutes in ice. After washing with PBS the slides were placed in a wet pan and 50 μL of the reaction mixture was added to each sample and then incubated at 37 °C for 60 minutes. The nuclei of cells were stained with DAPI and were further studied according to the procedure explained in the previous section.

TAOC assay

An assay kit for measuring the total antioxidant capacity (T-AOC) (Elabscience Biotechnology Inc.) was used to measure the TAOC of the compound 5g. The applied method is based on the inhibition of ABTS oxidation to the ABTS + by the studied compound. The concentration of

the ABTS + can be obtained by measuring the absorbance of ABTS + at 414 nm. The studied cells were collected, and after the addition of cold PBS, homogenized using an ultrasonic bath. The supernatant was transferred to a proper tube, and the reagent was added to the solutions. The absorbance intensities and the total protein concentration were recorded for all samples. The calculations were performed based on the kit provider's guidelines.

MDA assay

Biocore Diagnostik (ZellBio) MDA assay kit was used to assess lipid peroxidation. The method is based on the formation of MDA (Malondialdehyde) –TBA (thiobarbituric acid) adduct from the MDA-TBA reaction at high temperatures. Then MDA is measured in hot (90-100 °C) acidic media using colorimetric measurements at 532 (530-540 nm). In summary, after the preparation of the cell homogenate, the reagent was added to the samples, and the results were recorded and analyzed, as noted by the kit provider.

LDH assay

LDH release was measured using a CytoSelect LDH Assay Kit (Cell BioLabs, San Diego, CA) based on the standard protocol. PC12 cells were placed in the 96-well plates (1×10^4 cells/well) and cultivated 24 h before the experiment was performed. The cells were treated with Aβ1–42 (20 μM), with or without various concentrations of donepezil and compound 5g for 48 h. Then 90 μL of the supernatant was transferred to a well containing 10 μL LDH reagent and incubated for 30 min. The optical density was recorded at 450 nm using Epoch™ spectrophotometer (BioTek Instrument).

IL-1β and TNF-α gene expression analysis

SYBR Green method-based real-time PCR was used to measure mRNA level of the interleukin (IL)-1β, IL-6, and tumor necrosis factor-α (TNF-α) genes in PC12 cells. Total RNA (SinaClon, Tehran, Iran) was isolated using the RNX-PLUS solution. Revert Aid Reverse Transcriptase Kit (Thermo Fisher, Waltham, MA, USA) was used to synthesize the complementary DNA (cDNA). β-actin was utilized as an endogenous control for mRNA expression. The relative amount of gene expressions was calculated using the 2−ΔΔCT method. PC12 cells were treated with Aβ (5μM) and the level of the IL-1β and TNF-α genes was investigated in the presence and absence of the donepezil and compound 5g.

In vivo studies

Animals

Sixty adult male Wistar rats with the age of eight weeks and weight of 250-280 g were used for animal study. Standard cages exposed to a 12/12 h light/dark cycle at 23 ± 2 °C temperature were used to keep the animals. The access to the food was ad libitum. All experiments were done based on the Guide for the Care and Use of Laboratory Animals of the National Institute of Health (NIH; Publication No. 85–23, revised 1985). The Health Ministry ethically approved this study of the Islamic Republic of Iran under the grant number (No: 97015588) and the obtaining of the blood samples from a healthy volunteer was approved by local ethics (IR.TBZMED.REC.868).

Intracerebroventricular (i.c.v.) injection of Aβ1–42 peptides

$A\beta_{1-42}$ was dissolved in PBS (10 μM) and incubated for 4 days at 37 ℃ for peptide aggregation. Bilateral i.c.v. a stereotaxic apparatus did injection of obtained Aβ1–42 solution. To implant the sterile stainless steel guide cannula (26-gauge) in the injection sites, the rats were anesthetized by i.p. administrating ketamine–xylazine (90/10 mg/kg) solution. The injection site coordination was selected based on the rat brain in stereotaxic coordinates.[37] The position was located in the anteroposterior from bregma (AP) = -0.96, mediolateral from the midline (ML) = ± 2, and dorsoventral from the skull (DV) = 3.5.

An infusion pump was used to infuse $A\beta_{1-42}$ (50 pmol per animal) (10.3390/molecules22112007). The same protocol was utilized for Sham-operated animals, except for the injection of the vehicle instead all rats were individually housed following 1 day of surgery and then returned to the initial care state.

The rats were divided into 6 different groups (n = 10). Animals in sham surgery and AD groups received 1 ml/kg/day of normal saline via the oral route. Other animals in AD groups received donepezil (2 mg/kg/day) or compound 5g (1, 2, or 4 mg/kg/day) via a similar route for 21 days.

Morris water maze (MWM) protocol

To perform MWM studies, we used an apparatus in which the black circular pool (120 cm diameter and 60 cm height) of it filled with water (24–25 C, depth 30 cm). the pool was equipped with a 10 cm diameter submerged transparent escape platform that was placed 1 cm above (visible platform) or 1 cm below (hidden platform) the water level. Then, the pool was divided into four hypothetical quadrants for test start positions. Data were recorded using a video camera connected to a computerized tracking system (EthoVision XT). The camera was placed above the pool center.

Visible platform

The hidden platform was begun 1 day before the visual version of the water maze. To perform this experiment, the platform was marked by a beacon, and the rat was allowed to find the platform spontaneously within 60 s and left on the platform for 10 s. in the case the rat did not find that platform, it was firmly directed to the platform by

the investigator. The animals' performance on the visual platform task confirmed their good vision and motor and mental competence to do the task.

Hidden platform

The working memory could be evaluated using a hidden platform. The hidden platform was 1 cm below the water's surface. For the spatial learning (acquisition and probe trials) task, the time spent by the rat to find the platform was recorded as an escape latency time in each trial.

Probe test

Reference memory was evaluated a probe test was performed. To do this the next day after the last learning trial, a single probe trial was performed in which animals were allowed to freely swim without the platform for 60 s. The analysis of the probe trial shows the index of memory, in which the time spent in the platform quadrant was noted.

Novel object recognition (NOR) Test

A NOR test was done in 3 sessions (habituation, training, and retention) with moderate modifications. The Plexiglass open-field box (50 × 50 × 30 cm) and regular objects with various shapes and textures were utilized. The rat's nose direction to the object (distance of ≤ 2 cm) and rearing up against the object were noted as exploration. The total locomotor activity (in habituation session) and the spent time with each object were recorded using a video camera and scored using EthoVision XT video tracking software.

After placing the rats in the box without objects for 10 min for habituation. They were trained using 2 identical objects (A and A'). The total time spent exploring objects was recorded. In the retention session, the animals were returned to the same task by replacing one of the objects with a new object named B.

The discrimination index (DI) was calculated and utilized as an index of the recognition memory through the following equation.

$$DI = (N-F)/(N+F)$$

Where N stands for the time spent exploring the new object and F is the time spent exploring the familiar object in retention sessions.

Rat brain tissue sampling

After finalizing the behavioral test, brain tissues were removed for enzyme activity and cytokine level investigations. Before removing brain tissue, deeply anesthetized animals using i.p. injection of ketamine/xylazine (90/10 mg/kg) and decapitated. As soon as the brain tissue was removed, it was transferred on ice the hippocampal tissue was isolated. The isolated hippocampal tissue was frozen in liquid nitrogen and stored at −70 °C for further analysis.

Cholinesterase activity assay in the rat brain

The cholinesterase enzyme activity in rats treated with compound 5g was studied using the cholinesterase quantitative assay kit (HITACHI 917 / MODULAR P). To do this, the proper dilution of the tissue was done. The lysate supernatant was subjected to the reagent, which contains Butyrylthiocholine. Cholinesterase enzymes hydrolyze the butyrylthiocholine to thiocholine, which reduces the yellow $(Fe(CN)_6)^{3-}$ to the colorless $(Fe(CN)_6)^{4-}$. The results could be analyzed using colorimetric assays.

Measurement of the expression of proinflammatory cytokines (TNFα and NF-kB) and AChE in rat brain using western blot analysis

The expression of proinflammatory cytokines (TNF-α and NF-κB), AChE, and GADH in rat brains in the presence of compound 5g and donepezil was studied using western blot. The tissue samples were lysed and the lysates were centrifuged at 4 ℃ 12 000 rpm for 10 minutes protein concentration of supernatants was determined by the Bradford method. Bovine serum albumin was used as the standard protein. After mixing the samples with sample buffer (containing Tris, glycerol, β-mercaptoethanol, Bromo phenol blue, and SDS), they heated for 10 minutes in boiling water. The proper amount of protein extract was subjected to 12% SDS-PAGE gels and the resulting spots were transferred to a polyvinylidene fluoride (PVDF) membrane (Millipore, Billerica, MA, USA). The membrane was shaken 5 times (15 min) with the blocking agent (5% defatted milk powder in TBST [Tris-buffered saline-Tween 20]) at room temperature before the incubation with the primary antibody. After blocking the membrane, primary antibodies were incubated for 18 hours. The primary antibody was diluted with the blocking buffer. The primary antibodies were β-actin (sc-47778, 1:300) as internal standard, ACHE (E-AB-70014, 1:1000), NFκB-p65 (E-AB-22066, 1:1000), TNFα (SC-130349, 1:1000). The membrane was washed three times (15 min) with TBST and was incubated (75 min) with secondary antibodies (m-IgGκBP-HRP (sc-516102, 1:1000) and mouse anti-rabbit IgG-HRP (sc-2357, 1:1000)). Enhanced chemiluminescence (ECL) (Millipore, USA) was used for visualization. Optical density analysis was performed for semi-quantitative measurements.

Statistical analysis

The obtained data for all cell-based and animal studies were statistically analyzed using one-way ANOVA, two-way ANOVA, or post hoc analysis. GraphPad Prism software (GraphPad Software, La Jolla, CA, USA, www. graph pad. com) and Excel software were used to visualize graphs. $P < 0.05$ was considered to be statistically significant.

Results and Discussion

Synthesis of the quaternary ammonium derivatives

The synthetic route of the key intermediate is shown in Fig. 2. 4-flourobenzaldehyde (1a) reacted with various secondary amines (2a-f) by nucleophilic substitution reaction[31] and compounds 3a-f were produced. Then 1b-d, 3a-f, and 3h compounds reacted with 5, 6-dimethoxy-2, 3-dihydro-1*H*-inden-1-one. More details of the synthesis procedure optimization and characterization of the synthesized compounds could be found in our previous papers.[30,31]

We synthesized the designed compounds in the current study with a minor revision compared to our previous papers,[30,31] to avoid superfluous byproducts produced. We conducted the reaction at room temperature, using EtOH as the solvent and aqueous NaOH (10 %) as the base. The quaternary ammonium compounds (5g-i) were synthesized from (5f-h) reacting with methyl iodide. The details of the chemical characterization of two newly synthesized compounds (5g and 5i) using ^{13}C NMR, IR, and, ^{1}H NMR are presented in Fig. S1 (Supplementary file 1).

hAChE and hBuChE inhibitory activity of synthesized molecules

The anticholinesterase activity of the synthesized compounds was studied against hAChE and hBuChE. Compounds 5h, 5j, 5k, and 5l were practically insoluble in the applied solvents, and consequently, their inhibitory activity was not further evaluated.

The IC_{50} values (Table 1) of the studied compounds toward hAChE were in the range of 0.1-75 µM. Compound 5g (IC_{50} = 0.1 µM) possesses the highest hAChE inhibitory activity lower than donepezil (IC_{50} = 0.014 µM). In comparison with Galantamine (IC_{50} = 3 µM), which binds to the anionic site of the hAChE, compounds 5g (IC_{50} = 0.1 µM) and 5f (IC_{50} = 0.9 µM) possessed higher inhibitory activity.

Table 1. Inhibitory Activity of studied compounds, Inhibition mechanism, KI and Ki constants of the studied compounds

	IC_{50} (µM) hAChE	IC_{50} (µM) hBuChE	hAChE/ hBuChE	KI µM	Ki µM
5a	26	562	0.05	37	2.1
5b	64	501	0.13	170.0	78
5c	57.5	631	0.08	1000.0	47
5d	70	501	0.14	-	14
5e	55	398	0.14	51	13
5f	0.9	126	0.01	0.62	0.157
5g	0.1	4.00	0.02	0.29	0.017
5h	> 75	> 1000	-		
5i	6.0	> 1000	-	15	3.2
5j	> 10	> 1000	-		
5k	> 10	> 1000	-		
5l	> 10	> 1000	-		
Galantamine	3.0	31.6	0.009	0.84	0.090
Donepezil	0.014	5.25	0.002	0.0041	0.0081

hBuChE inhibitory evaluations showed that compound 5g inhibitory activity (IC_{50} = 4 µm) is higher than donepezil (IC_{50} = 5.25 µM) and Galantamine (IC_{50} = 31.6 µM). The selectivity index for hAChE to hBuChE inhibition was calculated for studied compounds, and the results (Table 1) showed that compound 5i possessed much higher selectivity toward hAChE than donepezil and other studied compounds. Compound 5g is almost inactive against hBuChE. Also, compound 5f was more selective toward hAChE in comparison with 5g.

Kinetic study results (Table 1) showed that the synthesized compounds possessed mixed non-competitive inhibition, except for compound 5d which showed competitive inhibition. According to the results, the inhibition constants (k_i) of compounds 5f and 5d were smaller than their non-competitive inhibition constant (ki′) values. This finding showed that the tendency of these compounds to bind to the active site is greater than the steric site. In addition, k_i values of compounds 5f and 5g were smaller than ki value of compound 5d, which shows the higher affinity of compounds 5f and 5g to the steric site. In conclusion, the better inhibitory activity of compounds 5f and 5g compared to compound 5d can result from their tendency to bind to both steric and active sites of enzymes. Double reciprocal plots and secondary plots of compound 5g inhibitory activity are shown in Fig. S2 (Supplementary file 1).

SAR analysis of the studied compounds' cholinesterase inhibitory activity

Incorporating the quaternary ammonium into the para position of the phenyl ring (compounds 5g and 5i) significantly increased ChE inhibitory activity. Comparing compounds 5i and 5g shows that when this quaternary ammonium is a part of the piperazine ring (5g), the inhibitory effect against both enzymes increase significantly. Corresponding non-quaternary amine substituted compounds (i.e. 5f and 5h), showed much less ChE inhibitory activity (Table 1). The comparison of compounds 5f and 5h confirmed the importance of the piperazine ring. Substitution of piperazine with morpholine (compound 5c) leads to a significant reduction in inhibition efficacy in both enzymes, which shows the importance of a positively charged moiety rather than a functional group with hydrogen bonding capability.

A similar range of activities for compounds 5a-e against both enzymes revealed that the presence of positive charge in the exact distance from the aromatic linker is vital for ChE inhibitory activity, replacing piperazine with piperidine moiety (compound 5a) leads to significant activity reduction (Table 1). This finding confirms

the importance of a positively charged moiety in this position.[38] This parameter also is much more critical than hydrophobic moieties or the size of the group, as it is evident from compound 5i, in which the ring is substituted with quaternary ammonium, while hAChE inhibitory activity is about 10 times more than compounds 5a-e which have a different ring in this position. Simultaneously, a significant reduction in hBuChE inhibitory activity of compound 5i shows a significant impact of hydrophobic interactions on the interaction of studied compounds with the hBuChE binding pocket. The same finding was approved by significantly reducing compound 5f activity against hBuChE compared with 5g, with one more methyl group. Also, the compounds' 5h-5l loss of action against hBuChE confirms the findings above of the importance of positive charge and hydrophobic groups for both enzymes.

Toxicity profiling of compounds 5g and 5f

The cytotoxicity of the compounds with higher hAChE inhibitory activity (5f and 5g) was studied using MTT assay on MCF7, B16 and PC12 cell lines, and the resulting LD_{50} values are represented in Table 2. Compounds 5g and 5f possessed lower cell growth inhibitory activity against MCF7 and B16 cells, comparing with donepezil, which revealed lower cell toxicity against both normal and cancerous human derived cell lines. Galantamine LD_{50} values toward studied cell lines were higher than the studied compounds. The obtained LD_{50} values for both studied compounds were significantly higher than their IC_{50} values toward hAChE and hBuChE.

Furthermore, we studied the effect of compounds 5g, 5f, donepezil and galantamine on PC12 cell viability and the results showed no significant effect on the viability of PC12 cells in the studied concentrations. Other studied reported similar results for donepezil and galantamine.[39,40]

Inhibition of Aβ-induced death of PC12 cells by compound 5g

The cytotoxic effect of Aβ aggregation in neuronal cells is one of the main hallmarks of AD. Attenuation of Aβ aggregates is an understudy strategy for developing anti-AD drugs.[41,42] One of the frequently applied *in vitro* models for studying the neuroprotective effect of drug candidates is PC12 cell death induced by $Aβ_{1-40}$.[43] The underlying mechanism of cell death due to the accumulation of Aβ aggregates is unknown, but some studies suggested the crosstalk between autophagy, Apoptosis, ROS production, and inflammation as probable mechanisms.[42,44] Autophagy modulation has been suggested as a target for AD drugs. The autophagy activation mediates neuroprotection against induced cytotoxicity by Aβ, oxidative stress and Apoptosis.[43,45] ROS role in developing neurological disorders have been described in different studies.[46] A rising number of studies indicate the transaction between ROS and autophagy as determinants in neuronal homeostasis modulation.[46] In recent years, drugs that modulate autophagy and apoptosis attracted much attention.[42,47]

Table 2. The effect of compounds 5f, 5g, donepezil, and galantamine on the cell viability of MCF7, B16, and PC12

Compound	MCF_7 (LD_{50} μM)	B_{16} (LD_{50} μM)	PC12 (LD_{50} μM)
5g	2.21	3.17	No growth inhibition*
5f	24.25	23.97	No growth inhibition*
Donepezil	0.06	0.36	No growth inhibition*
Galantamine	31.19	34.09	No growth inhibition*

LD_{50}: The concentration of compound that causes 50% of cell viability.
* No significant cell growth inhibition was observed in the studied concentrations.

To examine the multi-targeted capability of the compound 5g, we studied its neuroprotective effect against Aβ-induced PC12 cell death. PC12 cells were incubated with 5 μM Aβ (1-42) for 24h in the presence and absence of the compound 5g (0.1 and 1.0 μM).[48] Fig. 3 shows the transmission electron microscopy (TEM) images of the normal, Aβ treated, and Aβ + 5g treated PC12 cells. The normal PC12 cells (Fig. 3a) shapes are round, clear, spindle, and normally dispersed. Fig. 3b shows the decreased viability of PC12 cells after incubation with Aβ. Apoptotic bodies were seen easily; cells grew more slowly than normal cells. The morphology of the Aβ treated cells changed to be less clear and kept their spindle shape.[49] The addition of compound 5g at both concentrations (0.1 and 1.0 μM) reversed the Aβ induced cell death (Figs. 3c and 3d). The protection was increased at a higher concentration of compound 5g.

The prevention of Aβ-induced neurotoxicity may occur via different mechanisms such as acting as an antioxidant agent, attenuating neuroinflammation, reduction of Aβ fibril formation, inhibition of cell membrane damage, and other mechanisms.[42] The probable mechanism of the Aβ-induced cell death reduction by compound 5g was studied, and the results are reported in the following sections.

Compound 5g effect on oxidative stress

Oxidative stress is one of the AD hallmarks, and drugs with antioxidant activity are candidates for MTD anti-AD agents. The antioxidant activity of drugs is attributed to their capacity for biological system protection against ROS and reactive nitrogen species (RNS) damage. Total antioxidant activity (TAC) is the general ROS and RNS scavenging capacity. Acute oxidative stress can lead to the rapid up-regulation of autophagy via post-translational modifications of key autophagy regulators. ROS can induce single-strand DNA breaks in telomeric regions, resulting in collapsed replication forks, un-replicated single-stranded DNA, and telomeric loss. Also, ROS can target lipid double bonds that will lead to the

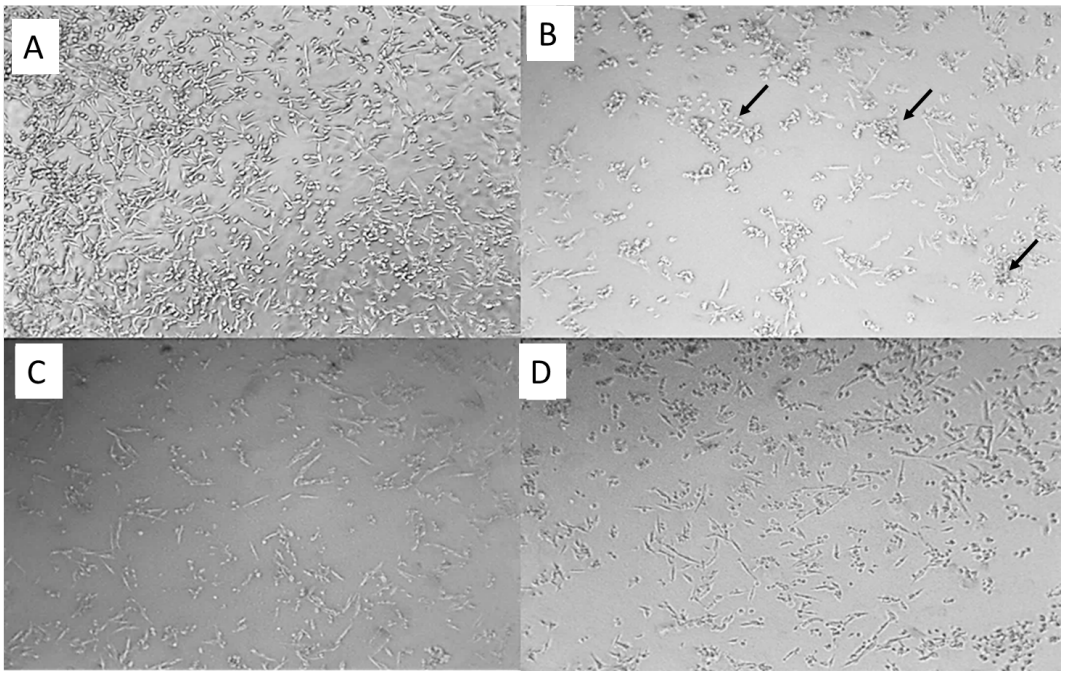

Fig. 3. TEM images of normal PC12 cells (a), Aβ treated PC12 cells (b), Aβ + 0.1 μM 5g, and Aβ + 1 μM 5g. Apoptotic bodies were shown by arrows.

production of reactive aldehydes like malondialdehyde (MDA) via the lipid-peroxidation procedure.[50] Reactive aldehydes can disrupt the cell membrane structure and function by interacting with membrane proteins, leading to neurotoxicity in the AD brain.[51,52] To examine the effect of compound 5g on Aβ induced death in PC12 cells via oxidative stress-related mechanisms, we studied compound 5g's effect on TAC, ROS production, and lipid peroxidation (MDA level).

Total antioxidant, anti-ROS production, and autophagy modulation capacity of compound 5g

We used dichlorofluorescein di-acetate (DCFH-DA) assay to measure the ROS level. Cellular esterases can convert nonpolar DCFH-DA (an oxidant-sensing fluorescent probe) to its polar derivative (DCFH). DCFH is a non-fluorescent moiety that intracellular ROS can oxidize to highly fluorescent DCF. Fig. 4A shows the images obtained using the fluorescence microscope for Aβ treated cells in the presence and absence of the compound 5g.

The counterstaining of the nuclei of the cells was done using 4′,6′-diamidino-2-phenylindole (DAPI). Using the DAPI staining, the cell nuclei along with the apoptotic bodies that include condensed and fragmented nuclei) can be illustrated (Fig. 4A). The nuclei of living or dead cells can emit blue fluorescence upon binding of DAPI to adenine–thymine regions of DNA. An increased number of cells with small, condensed nuclei after incubation with Aβ shows the enhancement of the apoptotic cells.

The morphological evaluation of DAPI stained cells (Fig. 4A) shows the capability of the compound 5g on the prevention of Aβ induced apoptosis. The apoptotic cells tend to lose cell structure. They also showed altered nuclear condensation. The control cells keep their intact and evenly shaped structures and nuclear condensation.

Fluorescence intensities (Fig. 4B) indicate the ROS level in the studied samples. Much intense green fluorescence of Aβ-treated cells compared to normal cells (Fig. 4A) shows enhanced production of ROS. The presence of the compound 5g leads to a reduction in ROS production. The DCF fluorescent intensity of the normal cells (20%) increased in Aβ treated cells (Fig. 4B). In contrast, compound 5g leads to less enhancement of the DCF fluorescent intensity. ROS reduction in the presence of the compound 5g could occur both via the radical scavenging property of compound 5g and autophagy modulation.

The total antioxidant activity of compound 5g was investigated using the fluorescein-based assay for oxygen radical absorbance capacity. As seen in Fig. 4C, the lowest absorbance of fluorescein was observed in Aβ-treated cells (69%), while in the presence of compound 5g (0.1 and 1 μM) the fluorescein absorbance was increased from to 74% and 87%, respectively. These results indicate the capability of the compound 5g for cell protection against Aβ-induced cell death partially via antioxidant activity.

Lipid peroxidation inhibitory effect of compound 5g and preventive effect of compound 5g on membrane damage

The capability of compound 5g for inhibiting lipid peroxidation was studied by measuring the MDA level in Aβ treated PC12 cells. Fig. 4D shows the MDA concentration in the studied cells. MDA levels were increased significantly in the $A\beta_{1-42}$ treated PC12 cells compared to control cells. The increased level of the MDA

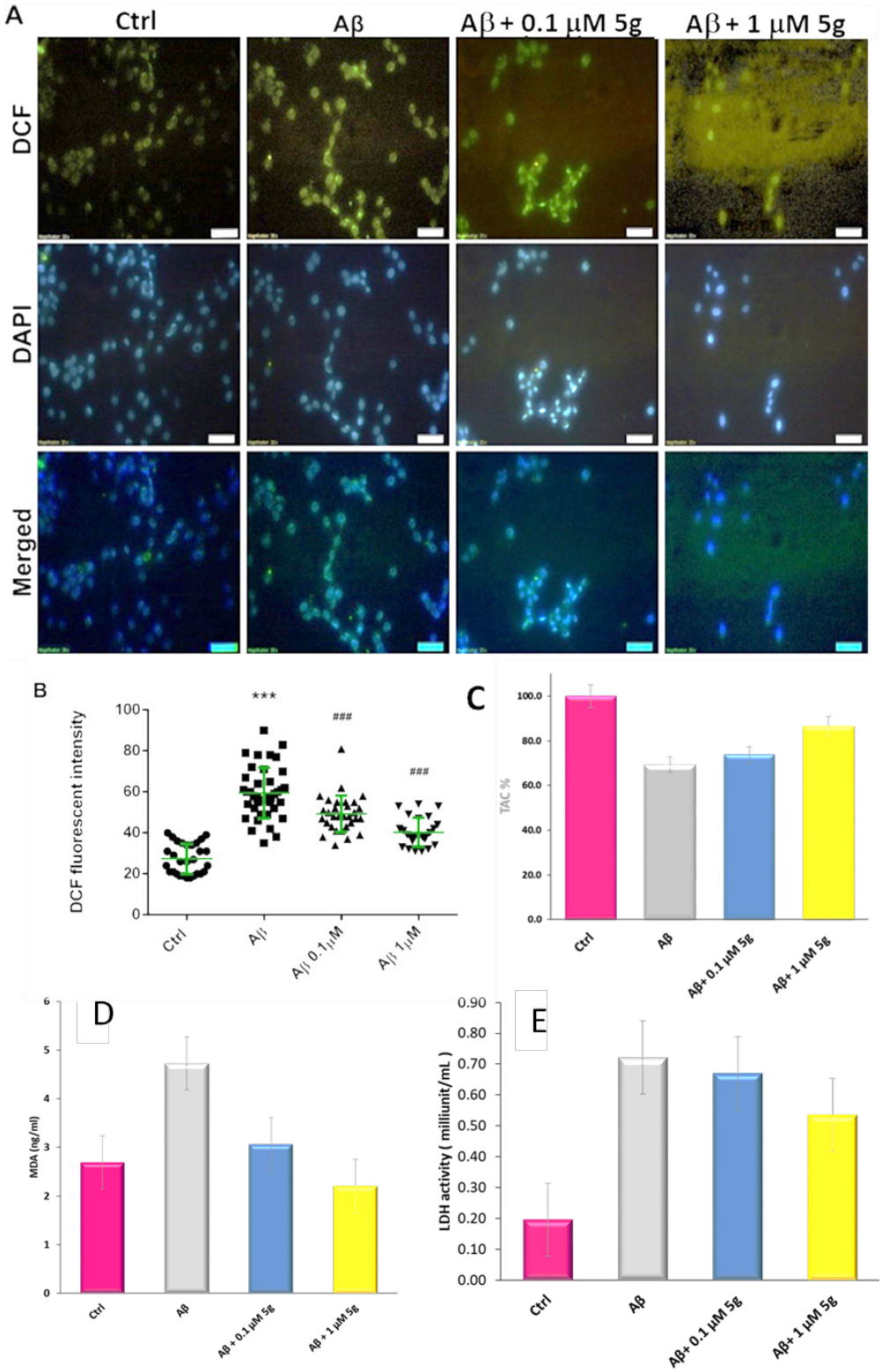

Fig. 4. Inhibition of ROS production by compound 5g in Aβ-induced neurotoxicity on PC12 cells. (A) The image of DCF and DAPI treated normal, Aβ and Aβ + compound 5g treated cells, (B) DCF fluorescent intensity of studied cells (C) TAC% of studied cells, (D) Lipid peroxidation and (E) and LDH activity

due to the $A\beta_{1-42}$, was reduced by the compound 5g. The results showed that the inhibition of lipid peroxidation plays a role in compound 5g prevention against Aβ induced cell death.

Plasma membrane damage is one of the key features of different forms of cellular damage, such as apoptosis and necrosis. Lactate dehydrogenase (LDH) is rapidly released into the cell culture supernatant via the damaged plasma membrane.[53] Also, the intracellular LDH level is a measure of cell viability. LDH activity is significantly

increased from about 20% in normal cells, to73.6% in Aβ treated cells (Fig. 4E). This finding suggests that the oxidative modification by Aβ (1-42) contributes to the impaired function of the PC12 cells. The compound 5g reduced LDH levels at both studied concentrations (68% for 0.1 μM and 55% for 1.0 μM). It could be concluded that the compound 5g contributes to preventing cellular membrane damage mechanisms. As mentioned, cellular membrane damage could occur via different mechanisms due to different pathway activations such as oxidative stress, apoptosis, autophagy, and other mechanisms.

The effect of compound 5g on DNA fragmentation and morphology of the apoptotic cells

The degree of the DNA fragmentation and morphology of the apoptotic cells were studied using a TUNEL assay. Apoptosis index for the normal cells and Aβ treated cells in the presence and the absence of the compound 5g are shown in Fig. 5A. The counterstained nuclei by DAPI and merged images are presented as well. The intense green color in the Aβ treated cells compared with control cells shows that the Aβ cell toxicity happens partly via an apoptotic mechanism. The apoptotic index (percentage of the apoptotic cells, Fig. 5B) increased from about 18% in control cells to 60% in the Aβ treated cells. The addition of the compound 5g to the incubation medium reduced the apoptotic index from 60% to 35% and 25% for the compound 5g concentration of 0.1 and 1.0 μM, respectively.

The TUNEL assay also revealed apoptotic characteristics in Aβ treated cells. The untreated cells showed blurred coloration, while apoptotic cells were stained by the TUNEL reagent (Fig. 5A). These results indicate the apparent DNA fragmentation and apoptotic nuclei. Also, the morphological variation and loss of cell integrity of apoptotic cells are apparent compared to the normal cells.

Compound 5g could prevent Aβ induced apoptosis by preventing both loss of cell integrity and DNA fragmentation. Cell membrane integrity loss is a hallmark of necrotic cell death, suggested as a player in neurodegenerative disease. According to the results, it could be concluded that compound 5g prevents PC12 cell death by contributing to oxidative stress, autophagy, apoptosis, and maybe necrosis. It also reduces radicals, prevents lipid peroxidation, and inhibits cell membrane damage.

Effect of compound 5g on neuro-inflammation

Activated microglia mediates the Aβ peptide-based neuroinflammation. IL-1β, IL-6, and TNF-α are pro-inflammatory cytokines that can be increased following the microglia activation and could influence the brain tissue and play a role in neurodegeneration as well as in neuroprotection.[54] Anti-inflammatory compounds that could reduce the expression of TNF-α and IL-1β have been investigated for their anti-AD potencies.[7] We studied the expression of mRNA levels of TNF-α and IL-1β in the presence and absence of compound 5g and donepezil. The mRNA level of IL-1β and TNF-α in Aβ treated PC12 cells increased compared to normal cells (Fig. 5C). Also, compound 5g prevented the enhancement of the IL-1β and TNF-α mRNA levels. The reduced levels of IL-1β and TNF-α mRNA could result from the Aβ induced cell toxicity at compound 5g concentrations of 0.1 μM ($P=0.0272$ for IL-1β and $P=0.01$ for TNF-α) and 1 μM ($P=0.0002$ for IL-1β and $P=0.0002$ for TNF-α). Furthermore, decreased expression levels of these genes were observed in compound 5g (1 μM) treated cells compared to control cells ($P=0.0397$ for IL-1β and $P=0.0478$ for TNF-α). The results are illustrated in Fig. 5 and Table 3. According to the results compound, 5g is capable of decreasing inflammatory gene expression in its potency increases at higher doses. These findings suggested an anti-inflammatory mechanism for the compound 5g in addition to other pharmacological effects.

In vivo anti-Alzheimer efficacy of compound 5g

Effect of the compound 5g on the recognition function of Aβ induced AD rats

The capability of the compound 5g on the recognition function of rats was studied using the novel object recognition (NOR) task. NOR measures a specific form of recognition memory, and it has been increasingly used as an experimental tool in assessing drug effects on memory. The results of the NOR test (Fig. 6) revealed that there is no significant difference among studied groups in the locomotor activity ($P=0.39$) and total observation time ($P=0.77$) (Fig 6A and 6B). such finding approves the reliability of the task results for episodic memory. It also shows that the task results are independent of locomotor or observation biases. The discrimination index (DI) factor is an episodic-like memory index that was calculated for the studied groups, and the results indicated that the DI between groups is significantly different ($P<0.001$). DI was reduced in the normal saline group ($P<0.001$), which indicates the impairment of episodic-like memory. Furthermore, a significant increase of DI in donepezil ($P<0.01$) and compound 5g (1 μM) treated groups ($P<0.001$) (Fig. 6C) was observed, which could be an indicator of the protective effect of donepezil and compound 5g against episodic-like memory impairment.

According to the results, it could be concluded that although compound 5g includes a permanently charged amino group, it reaches the brain of AD rats. As mentioned in the introduction, a choline transporter has been suggested to transport the permanently charged molecules to the brain. As can be seen from the results (Fig. 6C), by increasing the compound 5g dose from 0.5 to 1 μM, a noticeable improvement was observed in the

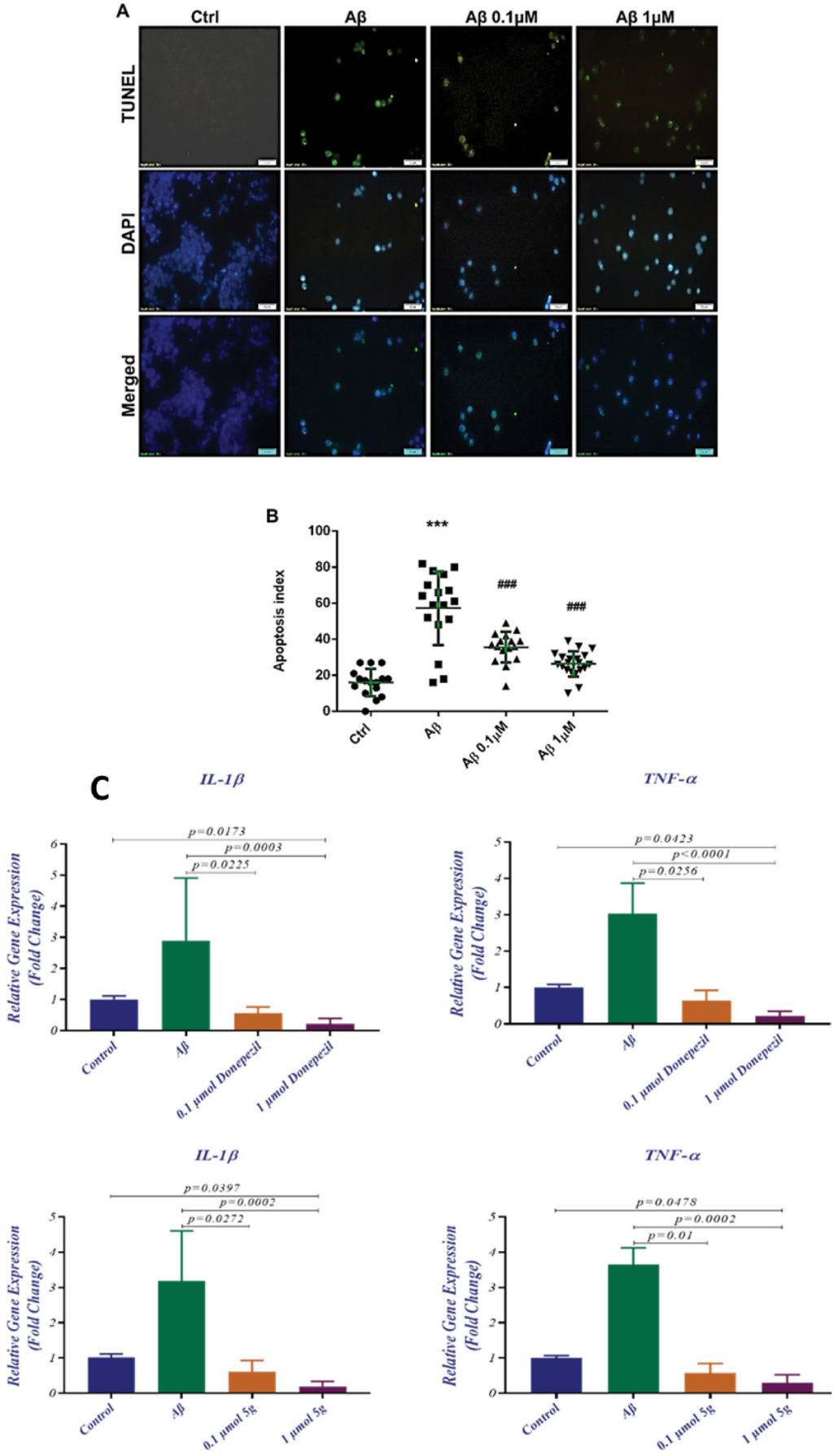

Fig. 5. Compound 5g effect on Aβ-induced apoptosis investigated by (A) TUNNEL assay and DAPI counterstaining and (B) DCF fluorescent intensity, (C) the effect of compound 5g and donepezil on the inflammatory genes' expression

Table 3. Effect of the compound 5g and donepezil on neuro-inflammatory gene expression in PC12 cells treated with Aβ

Target Gene	Control Mean ± SD (G1)	Aβ Mean ± SD (G2)	0.1 µM 5g Mean ± SD (G3)	1 µM 5g Mean ± SD (G4)	*P* value					
					G1 vs G2	G1 vs G3	G1 vs G4	G2 vs G3	G2 vs G4	G3 vs G4
IL-1β	1.012 ± 0.0986	3.178 ± 1.422	0.6117 ± 0.3142	0.1917 ± 0.1493	N	N	0.0397	0.0272	0.0002	N
TNF-α	1.002 ± 0.0646	3.648 ± 0.473	0.58 ± 0.2635	0.29 ± 0.239	N	N	0.0478	0.0100	0.0002	N
	Control Mean ± SD (G1)	Aβ Mean ± SD (G2)	1 µM Donepezil Mean ± SD (G3)	10 µM Donepezil Mean ± SD (G4)	G1 vs G2	G1 vs G3	G1 vs G4	G2 vs G3	G2 vs G4	G3 vs G4
IL-1β	1.002 ± 0.1103	2.895 ± 2.018	0.5633 ± 0.2001	0.2083 ± 0.1857	N	N	0.0173	0.0225	0.0003	N
TNF-α	1.012 ± 0.0716	3.038 ± 0.8302	0.6333 ± 0.2901	0.2267 ± 0.1253	N	N	0.0423	0.0256	< 0.0001	N

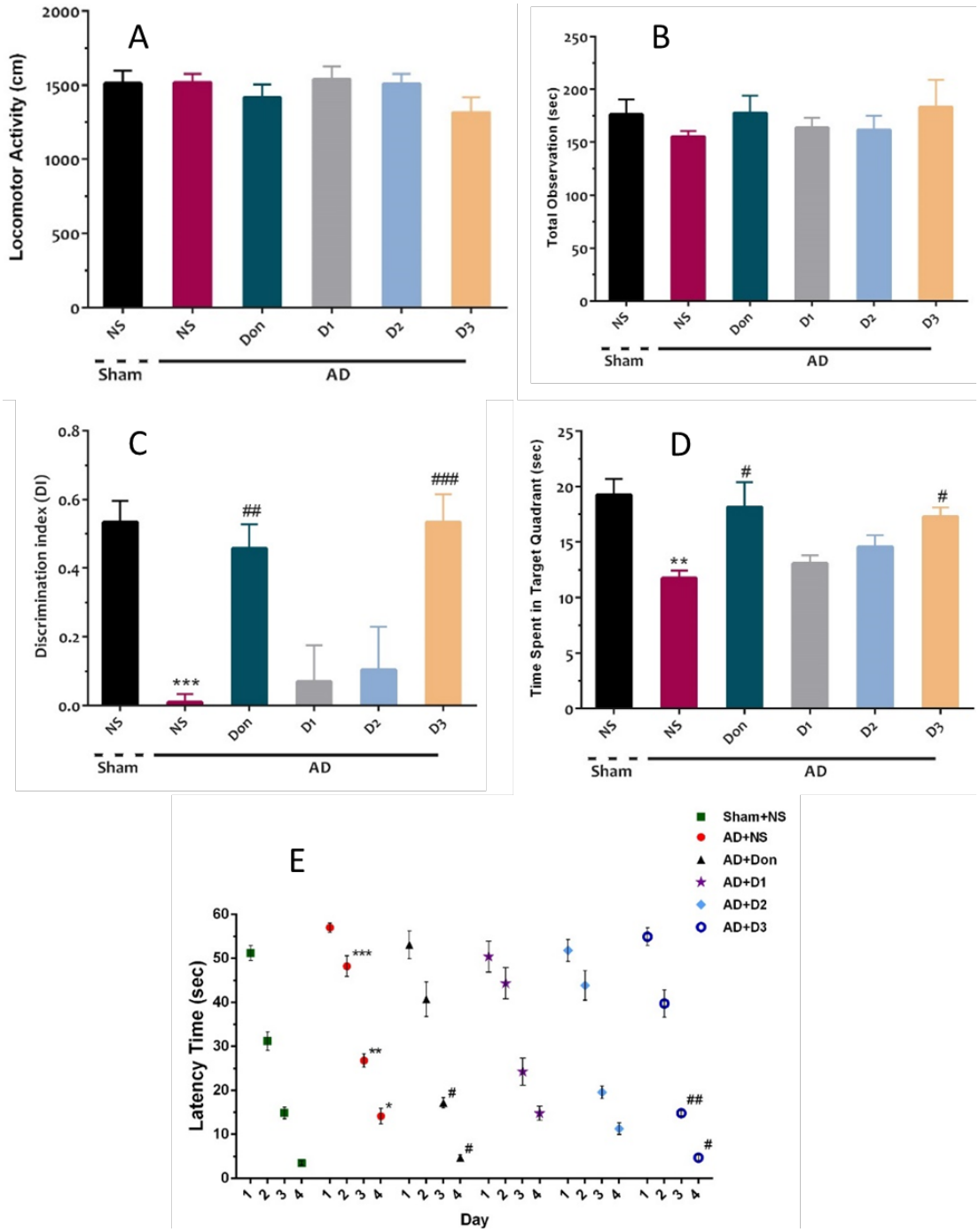

Fig. 6. (A) Mean locomotor activity, (B) total observation time, and (C) displacement index (DI) in the NOR task in different groups. (D) Time spent in target quadrant and (E) Mean escape latencies during 4 days of training sessions of MWM in different groups. Each bar represents the mean ± SEM, (n = 10). *** *P* < 0.001 compared with the sham. ## *P* < 0.01 and ### *P* < 0.001 compared with the AD + NS

recognition function of rats. This could result from the role of a transporter in compound 5g transportation to the brain. As we used the Aβ model of AD, and Aβ has been suggested as an inhibitor of the choline transporter, the significantly lower efficacy at lower concentrations of compound 5g could result from their disability to reach the brain due to the inhibition of the choline transporter. Moreover, the efficacy of compound 5g in the improvement of the cognition function of AD rats is comparable with donepezil (0.5 μM) as a positive control. Due to the probable dependence of compound 5g transportation to the brain to choline transporter and its inhibition by Aβ, its application of albumin may lead to different results.

Effect of the compound 5g on the spatial learning and memory function of Aβ induced AD rats

In addition, we conducted a Moris water maze (MWM) test to investigate the spatial learning and memory function of Aβ-induced AD in rats. The escape latency time was studied during the training days in control and treated groups. The comparison of the results showed that there are significant effects of day and group ($P<0.001$), as well as group × day ($P=0.04$). Such results indicated that even though animals learned the task across training days, different learning outcomes were observed among groups. Furthermore, post hoc analysis of the obtained results revealed a more extended escape latency time for the normal saline-treated group in the 2-4 days of the training session ($P<0.001$, $P<0.01$, and $P<0.05$, respectively), which shows the lower target-platform finding ability of animals in this group. Furthermore, escape latency times on the 3rd and fourth days were significantly decreased in the presence of donepezil and compound 5g ($P<0.05$ or $P<0.01$) (Fig. 7D). Also, the time spent to find the target quadrant was significantly different between groups in the probe session ($P<0.001$). The time spent in the target quadrant was different between sham and normal-saline-treated groups ($P<0.01$), which confirms spatial memory impairment. Also, a significant difference was observed between the normal-saline-treated group with donepezil and compound 5g (1 μM) treated groups ($P<0.05$) groups (Fig. 7E).

Effect of compound 5g on the expression of proinflammatory cytokines (TNFα and NF-κB) in Aβ-induced AD rat brain

We used the western blot analysis of the hippocamp tissue biopsy obtained from AD rats' brains to investigate the effect of compound 5g on the proinflammatory cytokines

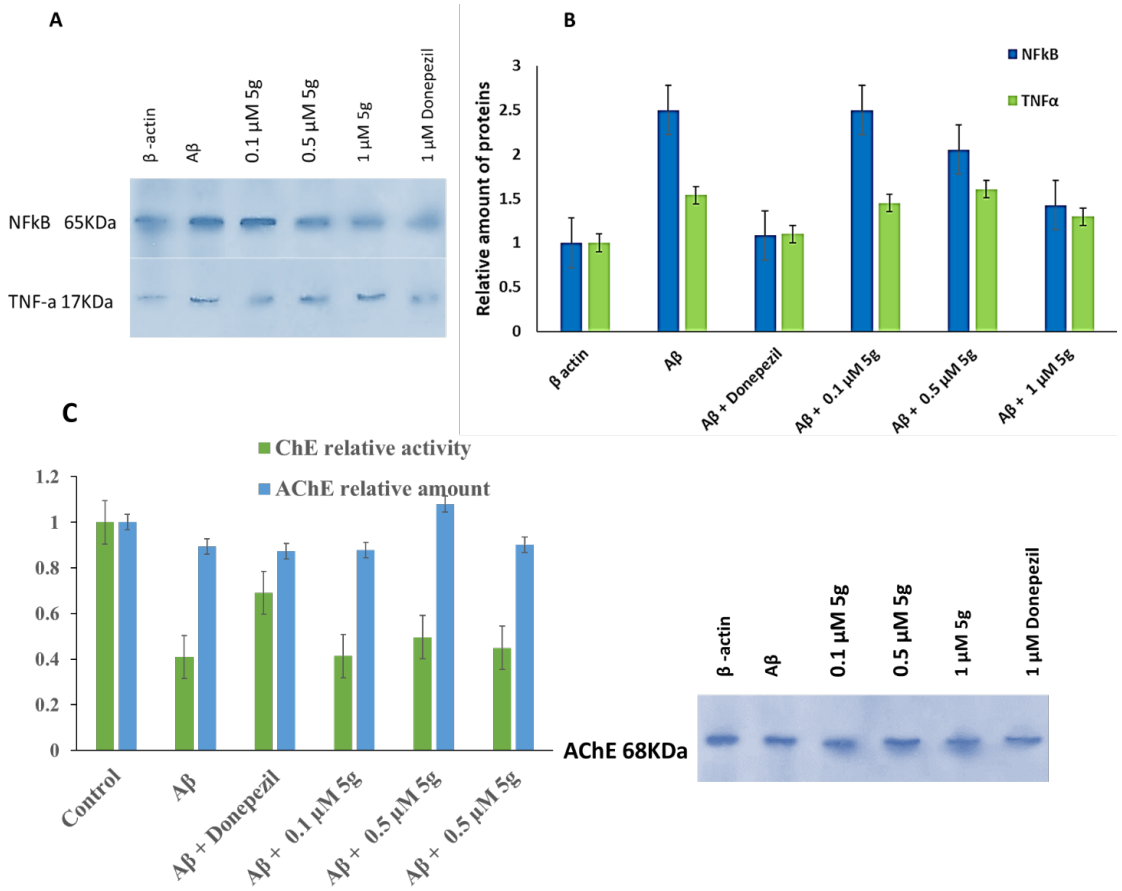

Fig. 7. Effect of compound 5g on the expression of proinflammatory cytokines (TNFα and NF-κB), and GADH in AD rats' hippocamp SDS-PAGE results (A) and relative amount of protein (B), Effect of compound 5g on the AChE relative amount and ChE relative activity in AD rats' hippocamp (C)

(TNFα and NF-κB) level. Minor downregulation of TNFα in hippocamp tissue was observed in compound 5g treated AD rats' brains (Fig. 7C). We showed a significant reduction in TNFα mRNA expression in Aβ + compound 5g treated PC12 cells. NF-κB was downregulated due to the compound 5g administration significantly in a dose-dependent manner (Fig. 7C). Activated NF-κB regulates the expression of COX2 enzyme, TNF, IL-1, IL-6, and IL-8 cytokines, adhesion, and cell cycle regulatory molecules.[42] The compound 5g mediated reduction of NF-κB may result in neuroinflammation modulation of neuronal cells. Downregulation of NF-κB and TNFα was observed in donepezil-treated AD rats' hippocamp (Fig. 7C).

Effect of compound 5g on total ChE activity and AChE level in rat brain

It is well known that the ChE activity and expression show a diverse correlation with inhibitors and physiologic conditions such as variations in Aβ precursor's level. It has been reported previously that the Aβ treated neuronal cells show downregulation of AChE expression. Also, some studies reported that Aβ could enhance the ChE hydrolyzing activity, resulting from the formation of soluble ultra-reactive acetylcholine-hydrolyzing Aβ-ChE complexes.[55] Our results showed that the Aβ treatment reduces the ChE activity and downregulation of AChE in the rat brain. The reduction of ChE activity can result from its downregulation or complex formation with Aβ.

To evaluate the compound 5g effects on the ChE activity in the Aβ-treated rat's brain, the butyrylthiocholine concentration was measured using a colorimetric method. Moreover, the AChE level was quantitatively measured using the western blot method. The results are shown in Fig. 8.

According to the results compound, 5g (0.5 μM) prevented the downregulation of AChE in Aβ-received rats' brains. Compound 5g also decreased ChE activity compared to the control group (Fig. 8), while the activity reduction was less than Aβ treated group and more than the donepezil-treated group.

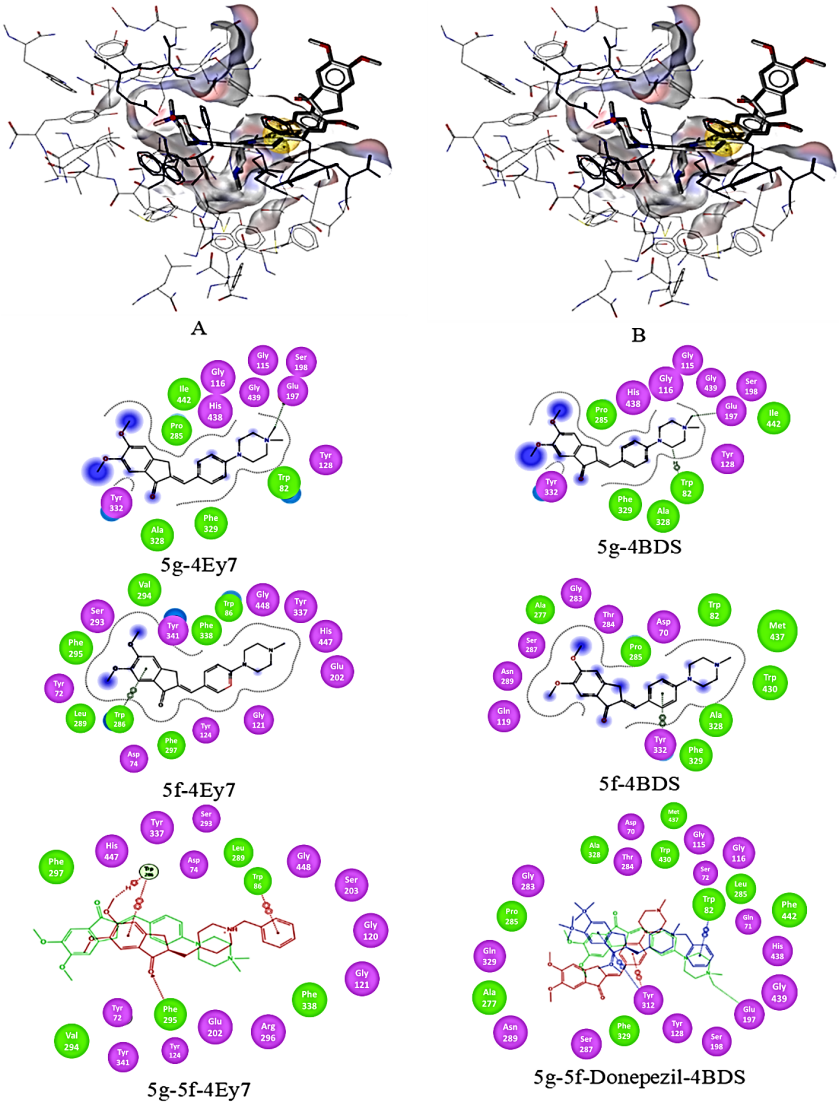

Fig. 8. Binding pose of compounds 5g and 5f docked to the binding cavity of hAChE (4Ey7) (A) and hBuChE (4BDS) (B) along with 2D illustration of complexes.

Donepezil could not prevent the Aβ induced downregulation of AChE while it inhibited the ChE activity reduction due to Aβ. Compound 5g (0.1) almost completely reversed the regulation profile of AChE, while its effect on ChE activity was not significant compared with the Aβ-treated group at all studied doses. ChE activity reduction due to compound 5g could result from ChE inhibition by it. The prevention of downregulation of AChE could result from non-ChE inhibitory anti-AD effects of compound 5g, which was investigated and reported in this study.

These results could be due to the differences in the ChE inhibition mechanism of donepezil and compound 5g in a way that donepezil possesses competitive inhibition while compound 5g possesses mixed non-competitive inhibition based on the kinetic studies. Furthermore, compound 5g is inactive against BuChE while donepezil inhibits both enzymes, which could be a reason for their different efficacy on the reversion of Aβ induced ChE activity and AChE expression variation.

Molecular docking analysis and pharmacophore mapping

To optimize and validate the docking procedure, donepezil was docked to the binding cavity and the results were compared with co-crystallized donepezil with hAChE (pdb code 4EY7). Fig. S3 (Supplementary file 1) shows the superimposition of docked donepezil on co-crystallized donepezil with hAChE. The developed docking procedure predicted the binding mode well and resulted in high geometric similarity to the ligand conformation observed in the crystal structure.

Active compounds were docked in the binding pocket of hAChE (pdb code 4EY7) and hBuChE (pdb code: 4BDS). The best conformer (highest score and best orientation) of each compound was further studied using MOE (add reference: Molecular operation environment v2019.0102, Chemical Computing Group, Montreal, Canada) and LigandScout[56] software to investigate ligand-protein interactions and pharmacophore mapping of them.

Fig. 8 shows the 3D illustration of the positioning of the compounds 5f and 5g in the binding cavity of hAChE and hBuChE. Three main structural characteristics of the binding pocket of hAChE and hBuChE (Fig. 1) are the availability of a deep narrow gorge (20 Å), the catalytic active (anionic) subsite (CAS) in conjunction with a choline-binding pocket (esteratic subsite) makes the catalytic machinery located in the bottom of the gorge beyond a peripheral acyl pocket[57] and an anionic site in the entrance of the binding gorge which is known as peripheral anionic site (PAS).

The structural features of AChE and BuChE binding sites are shown in Fig. 1. CAS of both enzymes consists of conserved amino acids known as a catalytic triad, i.e., Ser203, His447, Glu334 in hAChE, and Ser198, His438, Glu325 in hBuChE. The choline-binding pocket consists of Trp86, Phe330, and Tyr337 amino acids in hAChE and Trp82, Phe329, and Ala328 in hBuChE. The aliphatic moiety of inhibitors is interacting with Trp86/82. An oxyanion domain is near the choline-binding pocket, which is responsible for a hydrogen-bond network between substrate and enzyme. Conserved water molecules in this domain are taking part in this network. Also, there is a peripheral acyl binding pocket in both enzymes, consisting of different amino acids. The peripheral acyl binding pocket of hAChE includes Phe295 and Phe297 replaced by Leu286 and Val288 in hBuChE. PAS takes part in complex formation with Aβ and initiates the fibril formation. PAS of hAChE includes hydrophobic residues, i.e. Tyr72, Asp74, Tyr124, Trp286, Tyr337, which enables interactions with charged moieties of inhibitor compounds.[58] Blockers of PAS would inhibit the interaction of hAChE with Aβ and decrease consequent neurotoxicity.[59,60] PAS of hBuChE consists of Asp70, Phe298, and Try332, which like hAChE PAS interacts with positively charged substrates and guides them down the gorge to the catalytic triad.[61] The main difference between PAS in hAChE and hBuChE is the less acidic nature of the hBuChE PAS. Lack of aromatic residues in three subsites of the binding gorge; i.e., PAS, choline-binding pocket, and acyl binding pocket of hBuChE leads to the significantly larger gorge of hBuChE in comparison with hAChE.[62,63] which enables the catalysis of larger substrates. The difference between acyl pockets of these enzymes is one of the most valuable features for developing selective inhibitors against hAChE and hBuChe, while the similarities simultaneously facilitate dual inhibitor development.

The results show that the availability of a positive charge in an appropriate position facilitates interaction with Glu197 in hBuChE, and a π-cation interaction with Trp86 and Trp82 of hAChE and hBuChE, respectively. Also, a hydrophobic interaction of one of the methyl groups of compounds 5g piperazine ring with Trp86 and Trp82 of hAChE and hBuChE has been observed (Fig. 8) and could be a partial replacement of Donepezil phenyl ring interaction with those amino acids. In comparison with donepezil, compound 5g lacks one of the main interactions with Trp86 (i.e. π– π stacking with the phenyl ring of donepezil) in hAChE, which could be a reason for lower potency. At the same time, a firm contact (which could be a hydrogen bond rather than an ionic interaction) with Glu197 of hBuChE leads to a bit higher efficacy of compound 5g than donepezil. Recent studies suggested that Glu197, a conserved amino acid within cholinesterase enzymes, has a significant role in binding substrate/inhibitors with hBuChE binding sites.[64] Molecular docking studies of the interaction between hBuChE and the studied compounds compared with donepezil revealed that the compound 5g possesses

similar interactions with the binding pocket. In contrast, compound 5f lacks interaction with Trp82, resulting from one methyl group removal. Quaternary ammonium itself does not lead to this variation in interaction, as the results showed that the consequent amino moiety of the piperazine ring converted to the quaternary amino moiety due to ionization in physiologic pH.

The carbonyl moiety of the indanone ring in compound 5f interacts with catalytic triad amino acids of hAChE via hydrogen bonds.[65] Also, the indanone carbonyl group establishes a hydrogen bond with Phe295 backbone NH. The additional interaction with the acyl binding pocket of hBuChE is evident for both compounds. Benzidine group of compounds 5g and 5f interact with Tyr341 and Tyr332 of hAChE and hBuChE, respectively.

The flexibility of the CAS interacting fragment of the molecule is important to enable its movement through the bottleneck of the gorge, and the introduction of one double bond to the linker leads to the reduction of the possibility of compounds reaching the CAS. This rigidity leads to the apparent conformation orientation variation compared with donepezil for compounds 5g and 5f, which is presented in Fig. 8. This miss-orientation can be observed in both enzymes. Molecular docking simulation of donepezil interaction with hAChE revealed that placement of the donepezil in the active site is facilitated by a conformational change (90° bending), which leads to suitable orientation. At the same time, this miss-orientation leads to an extra interaction with both enzymes' acyl binding pocket, which is not available in donepezil.

Exploring the water molecules in the active site of both enzymes showed some conserved water molecules in hAChE binding gorge, which are necessary for the interaction. The results of molecular docking without removing those water molecules showed the possibility of hydrogen bonding between methoxy moieties and at least one water molecule in PAS. Investigation of the hAChE-donepezil complex shows one water molecule in the suitable distance for such an interaction in PAS. The results are consistent with the previous studies,[38] of which suggested conserved water molecules in similar situations. Also, according to the reported B-factors for those water molecules, they could be considered conserved. Our studies suggested no similar hydrogen bonding in PAS of hBuChE.

Interaction with the peripheral site inhibits the interaction of the hAChE with Aβ, and accordingly, the developed compounds can be regarded as dual inhibitors [38] hAChE-hBuChE inhibitors.

Conclusion

Indanone cationic analogs were synthesized and their structures were characterized using spectroscopic methods. ChE inhibitory activity was examined against hAChE and hBuChE. Compounds 5f and 5g, exhibited IC_{50} values of 0.9 and 0.1 μM against hAChE and 126 and 4 μM against hBuChE. Furthermore, all compounds showed mixed non-competitive inhibition mechanisms except compound 5d, which showed a competitive mechanism.

The molecular modeling studies showed that compound 5g interacts with both active and peripheral binding sites. In addition, the availability of permanent quaternary ammonium moiety on the compound 5g facilitates its interaction with the oxyanion hole, which may inhibit the formation of Aβ-hAChE complex and consequent aggregation promotion. Furthermore, compound 5g surpassed donepezil in hBuChE inhibitory activity. It also exhibited potent neuroprotective properties against Aβ-induced neurotoxicity. Its neuroprotective effects attributes, antioxidant, anti-ROS, anti-lipid peroxidation, LDH inhibition, antiapoptotic, and anti-neuroinflammatory activities, which were studied in Aβ-treated PC12 cells. In addition, *in vivo*, administration of compound 5g to Aβ-induced AD rats improved cognition, spatial memory, and learning function of rats. Complementary Western blot analyses of brain biopsies from the studied rats verified a reduction in NF-κB, elevation of AChE, and reduction in ChE activity.

In summation, compound 5g emerges as a potent candidate for the development of dual hAChE and hBuChE inhibitors with multi-faceted anti-AD properties. Its effective brain delivery and profound therapeutic implications are bolstered by robust in vivo evidence.

Acknowledgments

This work was supported by the National Institute for Medical Research Development, the health ministry of the Islamic Republic of Iran, under grant number 97015588.

Authors' Contribution

Conceptualization: Somaieh Soltani, Mohammad-Reza Rashidi.
Data curation: Hosna Karami, Somaieh Soltani.
Formal analysis: Somaieh Soltani, Mohammad-Reza Rashidi.
Funding acquisition: Somaieh Soltani, Mohammad-Reza Rashidi.
Investigation: Hosna Karami, Somaieh Soltani, Saeed Sadigh-Eteghad, Roghaye Nikbakht, Hanieh Farrokhi, Farzaneh Narimani, Reza Teimuri-Mofrad.
Methodology: Somaieh Soltani, Mohammad-Reza Rashidi.
Resources: Somaieh Soltani, Gerhard Wolber, Mohammad-Reza Rashidi.
Software: Somaieh Soltani.
Supervision: Somaieh Soltani.
Validation: Somaieh Soltani, Mohammad-Reza Rashidi.
Visualization: Hosna Karami, Somaieh Soltani.
Writing–original draft: Hosna Karami, Gerhard Wolber, Saeed Sadigh-Eteghad, Mohammad-Reza Rashidi.
Writing–review & editing: Somaieh Soltani, Saeed Sadigh-Eteghad.

Competing Interests

The authors declare no conflict of interest.

Ethical Statement

The Health Ministry ethically approved this study of the Islamic Republic of Iran under grant number 97015588, and the obtaining of

Research Highlights

What is the current knowledge?

- Multi-targeted drugs (MTD) are promising agents that can act as anti-AD disease-modifying agents.
- anti-AD disease-modifying agents' design is demanding due to the rapid growth of AD patients.

What is new here?

- Multi-target anti-AD compounds were designed and synthesized utilizing a modified synthesis method.
- The synthesized molecules' anti-cholinesterase activity and inhibition kinetics were investigated, and the results showed that Compound 5g (a cationic compound) possesses significant anticholinesterase activity.
- Compound 5g reversed Aβ treated PC12 cells' morphology alteration and reduced expression of IL-1β and TNF-α genes.
- Compound 5g possessed anti-oxidative stress activity, LDH inhibition, reduction of neuro-inflammation, prevention of autophagy-apoptosis, and maybe necrosis.
- Administration of compound 5g to Aβtreated rats improved their cognition function and spatial memory learning behavior. Also, TNF-α and NF-κB down-regulated in compound 5g treated AD rats' hippocamp.
- Compound 5g reversed the up-regulation of AChE in Aβ treated rats' hippocamp. Molecular modeling studies confirmed the interaction of compound 5g with both steric and catalytic sites ChE enzymes.

the blood samples from a healthy volunteer was approved by local ethics (IR.TBZMED.REC.868).

Funding

The Health Ministry ethically approved this study of the Islamic Republic of Iran under the grant number (NO: 97015588), and the obtaining of the blood samples from a healthy volunteer was approved by local ethics (IR.TBZMED.REC.868) under informed consent.

Supplementary files

Supplementary file 1 contains Tables S1-S3.

Refrences

1. Haghaei H, Aref Hosseini SR, Soltani S, Fathi F, Mokhtari F, Karima S, et al. Kinetic and thermodynamic study of beta-boswellic acid interaction with Tau protein investigated by surface plasmon resonance and molecular modeling methods. *Bioimpacts* **2020**; 10: 17-25. doi: 10.15171/bi.2020.03.
2. Haghaei H, Soltani S, Aref Hosseini SR, Rashidi MR, Karima S. Boswellic acids as promising leads in drug development against Alzheimer's disease. *Pharm Sci* **2021**; 27: 14-31. doi: 10.34172/ps.2020.25.
3. Tiwari S, Atluri V, Kaushik A, Yndart A, Nair M. Alzheimer's disease: pathogenesis, diagnostics, and therapeutics. *Int J Nanomedicine* **2019**; 14: 5541-54. doi: 10.2147/ijn.s200490.
4. Breijyeh Z, Karaman R. Comprehensive review on Alzheimer's disease: causes and treatment. *Molecules* **2020**; 25: 5789. doi: 10.3390/molecules25245789.
5. Khan S, Barve KH, Kumar MS. Recent advancements in pathogenesis, diagnostics and treatment of Alzheimer's disease. *Curr Neuropharmacol* **2020**; 18: 1106-25. doi: 10.2174/1570159x18666200528142429.
6. Ferrari C, Sorbi S. The complexity of Alzheimer's disease: an evolving puzzle. *Physiol Rev* **2021**; 101: 1047-81. doi: 10.1152/physrev.00015.2020.
7. Twarowski B, Herbet M. Inflammatory processes in Alzheimer's disease-pathomechanism, diagnosis and treatment: a review. *Int J Mol Sci* **2023**; 24: 6518. doi: 10.3390/ijms24076518.
8. Hampel H, O'Bryant SE, Molinuevo JL, Zetterberg H, Masters CL, Lista S, et al. Blood-based biomarkers for Alzheimer disease: mapping the road to the clinic. *Nat Rev Neurol* **2018**; 14: 639-52. doi: 10.1038/s41582-018-0079-7.
9. Unzeta M, Esteban G, Bolea I, Fogel WA, Ramsay RR, Youdim MB, et al. Multi-target directed donepezil-like ligands for Alzheimer's disease. *Front Neurosci* **2016**; 10: 205. doi: 10.3389/fnins.2016.00205.
10. Khoobi M, Alipour M, Moradi A, Sakhteman A, Nadri H, Razavi SF, et al. Design, synthesis, docking study and biological evaluation of some novel tetrahydrochromeno [3',4':5,6] pyrano[2,3-b]quinolin-6(7H)-one derivatives against acetyl- and butyrylcholinesterase. *Eur J Med Chem* **2013**; 68: 291-300. doi: 10.1016/j.ejmech.2013.07.045.
11. Colović MB, Krstić DZ, Lazarević-Pašti TD, Bondžić AM, Vasić VM. Acetylcholinesterase inhibitors: pharmacology and toxicology. *Curr Neuropharmacol* **2013**; 11: 315-35. doi: 10.2174/1570159x11311030006.
12. Bajda M, Guzior N, Ignasik M, Malawska B. Multi-target-directed ligands in Alzheimer's disease treatment. *Curr Med Chem* **2011**; 18: 4949-75. doi: 10.2174/092986711797535245.
13. Greig NH, Lahiri DK, Sambamurti K. Butyrylcholinesterase: an important new target in Alzheimer's disease therapy. *Int Psychogeriatr* **2002**; 14 Suppl 1: 77-91. doi: 10.1017/s1041610203008676.
14. Alvarez A, Opazo C, Alarcón R, Garrido J, Inestrosa NC. Acetylcholinesterase promotes the aggregation of amyloid-beta-peptide fragments by forming a complex with the growing fibrils. *J Mol Biol* **1997**; 272: 348-61. doi: 10.1006/jmbi.1997.1245.
15. Inestrosa NC, Sagal JP, Colombres M. Acetylcholinesterase interaction with Alzheimer amyloid beta. *Subcell Biochem* **2005**; 38: 299-317. doi: 10.1007/0-387-23226-5_15.
16. Mishra CB, Kumari S, Manral A, Prakash A, Saini V, Lynn AM, et al. Design, synthesis, in-silico and biological evaluation of novel donepezil derivatives as multi-target-directed ligands for the treatment of Alzheimer's disease. *Eur J Med Chem* **2017**; 125: 736-50. doi: 10.1016/j.ejmech.2016.09.057.
17. Stavrakov G, Philipova I, Zheleva D, Atanasova M, Konstantinov S, Doytchinova I. Docking-based design of galantamine derivatives with dual-site binding to acetylcholinesterase. *Mol Inform* **2016**; 35: 278-85. doi: 10.1002/minf.201600041.
18. Jouyban A, Soltani S. Blood brain barrier permeation. In: Acree W, ed. *Toxicity and Drug Testing*. Rijeka: IntechOpen; **2012**. doi: 10.5772/20360.
19. Clark JK, Cowley P, Muir AW, Palin R, Pow E, Prosser AB, et al. Quaternary salts of E2020 analogues as acetylcholinesterase inhibitors for the reversal of neuromuscular block. *Bioorg Med Chem Lett* **2002**; 12: 2565-8. doi: 10.1016/s0960-894x(02)00482-1.
20. Komloova M, Musilek K, Dolezal M, Gunn-Moore F, Kuca K. Structure-activity relationship of quaternary acetylcholinesterase inhibitors - outlook for early myasthenia gravis treatment. *Curr Med Chem* **2010**; 17: 1810-24. doi: 10.2174/092986710791111198.
21. Akaike A, Shimohama S, Misu Y. *Nicotinic Acetylcholine Receptor Signaling in Neuroprotection*. Singapore: Springer; **2018**. doi: 10.1007/978-981-10-8488-1.
22. Muramatsu I, Masuoka T, Uwada J, Yoshiki H, Yazama T, Lee KS, et al. A new aspect of cholinergic transmission in the central nervous system. In: Akaike A, Shimohama S, Misu Y, eds. *Nicotinic Acetylcholine Receptor Signaling in Neuroprotection*. Singapore: Springer; **2018**. p. 45-58. doi: 10.1007/978-981-10-8488-1_3.
23. Geldenhuys WJ, Allen DD, Lockman PR. 3-D-QSAR and docking studies on the neuronal choline transporter. *Bioorg Med Chem Lett* **2010**; 20: 4870-7. doi: 10.1016/j.bmcl.2010.06.090.
24. Kim MH, Maeng HJ, Yu KH, Lee KR, Tsuruo T, Kim DD, et al.

Evidence of carrier-mediated transport in the penetration of donepezil into the rat brain. *J Pharm Sci* **2010**; 99: 1548-66. doi: 10.1002/jps.21895.
25. Allen DD, Lockman PR. The blood-brain barrier choline transporter as a brain drug delivery vector. *Life Sci* **2003**; 73: 1609-15. doi: 10.1016/s0024-3205(03)00504-6.
26. Banks WA. Drug delivery to the brain in Alzheimer's disease: consideration of the blood-brain barrier. *Adv Drug Deliv Rev* **2012**; 64: 629-39. doi: 10.1016/j.addr.2011.12.005.
27. Rosenberry TL, Brazzolotto X, Macdonald IR, Wandhammer M, Trovaslet-Leroy M, Darvesh S, et al. Comparison of the binding of reversible inhibitors to human butyrylcholinesterase and acetylcholinesterase: a crystallographic, kinetic and calorimetric study. *Molecules* **2017**; 22: 2098. doi: 10.3390/molecules22122098.
28. Palin R, Clark JK, Cowley P, Muir AW, Pow E, Prosser AB, et al. Novel piperidinium and pyridinium agents as water-soluble acetylcholinesterase inhibitors for the reversal of neuromuscular blockade. *Bioorg Med Chem Lett* **2002**; 12: 2569-72. doi: 10.1016/s0960-894x(02)00483-3.
29. Mozaffarnia S, Parsaee F, Payami E, Karami H, Soltani S, Rashidi M-R, et al. Design, synthesis and biological assessment of novel 2-(4-alkoxybenzylidine)-2,3-dihydro-5,6-dimethoxy-1H-inden-1-one derivatives as hAChE and hBuChE enzyme inhibitors. *ChemistrySelect* **2019**; 4: 9376-80. doi: 10.1002/slct.201901973.
30. Teimuri-Mofrad R, Nikbakht R, Gholamhosseini-Nazari M. A convenient and efficient method for the synthesis of new 2-(4-amino substituted benzilidine) indanone derivatives. *Res Chem Intermed* **2016**; 42: 7501-11. doi: 10.1007/s11164-016-2549-0.
31. Rahimpour K, Nikbakht R, Aghaiepour A, Teimuri-Mofrad R. Synthesis of 2-(4-amino substituted benzylidene) indanone analogues from aromatic nucleophilic substitution (SNAr) reaction. *Synth Commun* **2018**; 48: 2253-9. doi: 10.1080/00397911.2018.1492726.
32. Berridge MV, Herst PM, Tan AS. Tetrazolium dyes as tools in cell biology: new insights into their cellular reduction. *Biotechnol Annu Rev* **2005**; 11: 127-52. doi: 10.1016/s1387-2656(05)11004-7.
33. Karimi G, Iranshahi M, Hosseinalizadeh F, Riahi B, Sahebkar A. Screening of acetylcholinesterase inhibitory activity of terpenoid and coumarin derivatives from the genus *Ferula*. *Pharmacologyonline* **2010**; 1: 566-74.
34. von Bernhardi R, Alarcón R, Mezzano D, Fuentes P, Inestrosa NC. Blood cells cholinesterase activity in early-stage Alzheimer's disease and vascular dementia. *Dement Geriatr Cogn Disord* **2005**; 19: 204-12. doi: 10.1159/000083500.
35. Gorun V, Proinov I, Baltescu V, Balaban G, Barzu O. Modified Ellman procedure for assay of cholinesterases in crude enzymatic preparations. *Anal Biochem* **1978**; 86: 324-6. doi: 10.1016/0003-2697(78)90350-0.
36. Rampa A, Bisi A, Belluti F, Gobbi S, Valenti P, Andrisano V, et al. Acetylcholinesterase inhibitors for potential use in Alzheimer's disease: molecular modeling, synthesis and kinetic evaluation of 11H-indeno-[1,2-b]-quinolin-10-ylamine derivatives. *Bioorg Med Chem* **2000**; 8: 497-506. doi: 10.1016/s0968-0896(99)00306-5.
37. Paxinos G, Watson C. *The Rat Brain in Stereotaxic Coordinates: Hard Cover Edition*. Elsevier; **2006**.
38. Peauger L, Azzouz R, Gembus V, Ţînţaş ML, Sopková-de Oliveira Santos J, Bohn P, et al. Donepezil-based central acetylcholinesterase inhibitors by means of a "bio-oxidizable" prodrug strategy: design, synthesis, and in vitro biological evaluation. *J Med Chem* **2017**; 60: 5909-26. doi: 10.1021/acs.jmedchem.7b00702.
39. Gao BL, Che NN, Li X, Ren CF. Neuroprotective effects of donepezil against Aβ25-35-induced neurotoxicity. *Eur J Med Res* **2022**; 27: 219. doi: 10.1186/s40001-022-00862-1.
40. Jiang S, Zhao Y, Zhang T, Lan J, Yang J, Yuan L, et al. Galantamine inhibits β-amyloid-induced cytostatic autophagy in PC12 cells through decreasing ROS production. *Cell Prolif* **2018**; 51: e12427. doi: 10.1111/cpr.12427.
41. Parsons CG, Rammes G. Preclinical to phase II amyloid beta (Aβ) peptide modulators under investigation for Alzheimer's disease. *Expert Opin Investig Drugs* **2017**; 26: 579-92. doi: 10.1080/13543784.2017.1313832.
42. Forest KH, Nichols RA. Assessing neuroprotective agents for Aβ-induced neurotoxicity. *Trends Mol Med* **2019**; 25: 685-95. doi: 10.1016/j.molmed.2019.05.013.
43. Tong Y, Bai L, Gong R, Chuan J, Duan X, Zhu Y. Shikonin protects PC12 cells against β-amyloid peptide-induced cell injury through antioxidant and antiapoptotic activities. *Sci Rep* **2018**; 8: 26. doi: 10.1038/s41598-017-18058-7.
44. Shanmuganathan B, Suryanarayanan V, Sathya S, Narenkumar M, Singh SK, Ruckmani K, et al. Anti-amyloidogenic and anti-apoptotic effect of α-bisabolol against Aβ induced neurotoxicity in PC12 cells. *Eur J Med Chem* **2018**; 143: 1196-207. doi: 10.1016/j.ejmech.2017.10.017.
45. Singh AK, Kashyap MP, Tripathi VK, Singh S, Garg G, Rizvi SI. Neuroprotection through rapamycin-induced activation of autophagy and PI3K/Akt1/mTOR/CREB signaling against amyloid-β-induced oxidative stress, synaptic/neurotransmission dysfunction, and neurodegeneration in adult rats. *Mol Neurobiol* **2017**; 54: 5815-28. doi: 10.1007/s12035-016-0129-3.
46. Fang C, Gu L, Smerin D, Mao S, Xiong X. The interrelation between reactive oxygen species and autophagy in neurological disorders. *Oxid Med Cell Longev* **2017**; 2017: 8495160. doi: 10.1155/2017/8495160.
47. Ghavami S, Shojaei S, Yeganeh B, Ande SR, Jangamreddy JR, Mehrpour M, et al. Autophagy and apoptosis dysfunction in neurodegenerative disorders. *Prog Neurobiol* **2014**; 112: 24-49. doi: 10.1016/j.pneurobio.2013.10.004.
48. Wei H, Leeds PR, Qian Y, Wei W, Chen R, Chuang D. beta-amyloid peptide-induced death of PC 12 cells and cerebellar granule cell neurons is inhibited by long-term lithium treatment. *Eur J Pharmacol* **2000**; 392: 117-23. doi: 10.1016/s0014-2999(00)00127-8.
49. Tian Z, Zhang X, Zhao Z, Zhang F, Deng T. The Wnt/β-catenin signaling pathway affects the distribution of cytoskeletal proteins in Aβ treated PC12 cells. *J Integr Neurosci* **2019**; 18: 309-12. doi: 10.31083/j.jin.2019.03.168.
50. Gęgotek A, Skrzydlewska E. Biological effect of protein modifications by lipid peroxidation products. *Chem Phys Lipids* **2019**; 221: 46-52. doi: 10.1016/j.chemphyslip.2019.03.011.
51. Cheignon C, Tomas M, Bonnefont-Rousselot D, Faller P, Hureau C, Collin F. Oxidative stress and the amyloid beta peptide in Alzheimer's disease. *Redox Biol* **2018**; 14: 450-64. doi: 10.1016/j.redox.2017.10.014.
52. Huang WJ, Zhang X, Chen WW. Role of oxidative stress in Alzheimer's disease. *Biomed Rep* **2016**; 4: 519-22. doi: 10.3892/br.2016.630.
53. Kumar P, Nagarajan A, Uchil PD. Analysis of cell viability by the lactate dehydrogenase assay. *Cold Spring Harb Protoc* **2018**; 2018: pdb.rot095497. doi: 10.1101/pdb.prot095497.
54. Wang WY, Tan MS, Yu JT, Tan L. Role of pro-inflammatory cytokines released from microglia in Alzheimer's disease. *Ann Transl Med* **2015**; 3: 136. doi: 10.3978/j.issn.2305-5839.2015.03.49.
55. Wang H, Zhang H. Reconsideration of anticholinesterase therapeutic strategies against Alzheimer's disease. *ACS Chem Neurosci* **2019**; 10: 852-62. doi: 10.1021/acschemneuro.8b00391.
56. Wolber G, Langer T. LigandScout: 3-D pharmacophores derived from protein-bound ligands and their use as virtual screening filters. *J Chem Inf Model* **2005**; 45: 160-9. doi: 10.1021/ci049885e.
57. Dvir H, Silman I, Harel M, Rosenberry TL, Sussman JL. Acetylcholinesterase: from 3D structure to function. *Chem Biol Interact* **2010**; 187: 10-22. doi: 10.1016/j.cbi.2010.01.042.
58. Johnson G, Moore SW. The peripheral anionic site of acetylcholinesterase: structure, functions and potential role in rational drug design. *Curr Pharm Des* **2006**; 12: 217-25. doi: 10.2174/138161206775193127.
59. Korabecny J, Spilovska K, Mezeiova E, Benek O, Juza R, Kaping D, et al. A systematic review on donepezil-based derivatives as

potential cholinesterase inhibitors for Alzheimer's disease. *Curr Med Chem* **2019**; 26: 5625-48. doi: 10.2174/0929867325666180517094023.
60. Li Q, Yang H, Chen Y, Sun H. Recent progress in the identification of selective butyrylcholinesterase inhibitors for Alzheimer's disease. *Eur J Med Chem* **2017**; 132: 294-309. doi: 10.1016/j.ejmech.2017.03.062.
61. Macdonald IR, Martin E, Rosenberry TL, Darvesh S. Probing the peripheral site of human butyrylcholinesterase. *Biochemistry* **2012**; 51: 7046-53. doi: 10.1021/bi300955k.
62. Saxena A, Redman AM, Jiang X, Lockridge O, Doctor BP. Differences in active site gorge dimensions of cholinesterases revealed by binding of inhibitors to human butyrylcholinesterase. *Biochemistry* **1997**; 36: 14642-51. doi: 10.1021/bi971425+.
63. Pezzementi L, Nachon F, Chatonnet A. Evolution of acetylcholinesterase and butyrylcholinesterase in the vertebrates: an atypical butyrylcholinesterase from the medaka *Oryzias latipes*. *PLoS One* **2011**; 6: e17396. doi: 10.1371/journal.pone.0017396.
64. Rosenberry TL, Brazzolotto X, Macdonald IR, Wandhammer M, Trovaslet-Leroy M, Darvesh S, et al. Comparison of the binding of reversible inhibitors to human butyrylcholinesterase and acetylcholinesterase: a crystallographic, kinetic and calorimetric study. *Molecules* **2017**; 22: 2098. doi: 10.3390/molecules22122098.
65. Cheung J, Rudolph MJ, Burshteyn F, Cassidy MS, Gary EN, Love J, et al. Structures of human acetylcholinesterase in complex with pharmacologically important ligands. *J Med Chem* **2012**; 55: 10282-6. doi: 10.1021/jm300871x.